

461362

CATALOGED BY: DDC

461362

AS AD NO.

FUEL CELL CATALYSTS

REPORT NO. 4

CONTRACT NO. DA-36-039 AMC-03700 (E)
TASK NO. 1G6 22001 A 053-04

FINAL REPORT

FOR THE PERIOD

1 DECEMBER 1963 - 30 NOVEMBER 1964

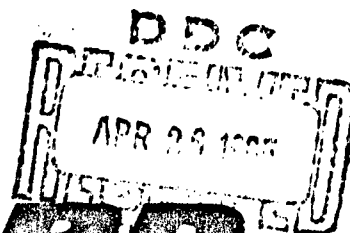
U.S. ARMY ELECTRONICS LABORATORIES
FORT MONMOUTH, NEW JERSEY

ENGELHARD

I N D U S T R I E S , I N C.

RESEARCH AND DEVELOPMENT DIVISION

NEWARK, NEW JERSEY



19990413025

NOTICE: When government or other drawings, specifications or other data are used for any purpose other than in connection with a definitely related government procurement operation, the U. S. Government thereby incurs no responsibility, nor any obligation whatsoever; and the fact that the Government may have formulated, furnished, or in any way supplied the said drawings, specifications, or other data is not to be regarded by implication or otherwise as in any manner licensing the holder or any other person or corporation, or conveying any rights or permission to manufacture, use or sell any patented invention that may in any way be related thereto.

QUALIFIED REQUESTORS MAY OBTAIN
COPIES OF THIS REPORT FROM DDC.
DDC RELEASE TO OTS NOT AUTHORIZED.

ENGELHARD
INDUSTRIES INC.

RESEARCH & DEVELOPMENT DIVISION
457 DELANCY STREET, NEWARK, NEW JERSEY
TELEPHONE: AREA CODE 201-242-3700

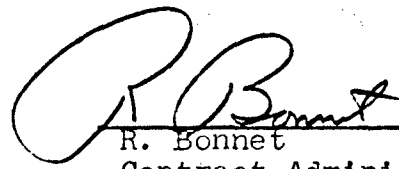
April 6, 1965

Gentlemen:

Enclosed please find a copy of the Final Quarterly Report under Contract DA-36-039 AMC-03700(E) issued to Engelhard Industries, Inc., Research and Development Division. This report is being distributed as per the distribution list submitted to us by the U.S. Army Electronics Laboratories, Fort Monmouth, New Jersey.

Yours sincerely,

ENGELHARD INDUSTRIES, INC.


R. Bonnet
Contract Administrator

RB/edm
Enclosure

FUEL CELL CATALYSTS

REPORT NO 4

Contract No. DA-36-039 AMC-03700(E)

Task No. 1G6 22001 A 053-04

FINAL REPORT

1 December 1963 - 30 November 1964

Object: To conduct research on electrode catalysts for operation of fuel cells in acid or neutral media employing liquid organic fuels and oxygen

Written by:

O. J. Adlhart
O. J. Adlhart

M. M. Hartwig
M. M. Hartwig

Approved by:

G. J. Cohn
G. J. Cohn

TABLE OF CONTENTS

	<u>Page</u>
Title Page	i
Table of Contents	ii
List of Tables	iv
List of Figures	vi
I. Purpose	1
II. Abstract	2
III. Publications, Lectures, Reports and Conferences	3
IV. Factual Data	4
A. Experimental Techniques for Catalyst Evaluation	4
1. Physical Measurements on Catalysts	4
a. Determination of Surface Area, Crystallite Size and Bulk Density on Bulk Catalysts	4
b. Measurement of Pore Size Distribution	4
c. Coulometric Surface Area Determination	4
2. Electrochemical Evaluation of Catalysts	8
a. Catalyst Evaluation by Transient Techniques	8
b. Current-Potential Measurements	9
B. Unsupported Platinum Metal Catalysts	11
1. Physical Properties of Unsupported Platinum Metal Blacks	12
a. Pure Metal Blacks	12
b. Alloys Blacks of Platinum with Ruthenium, Rhodium and Iridium	13
2. Anodic Performance of Unsupported Platinum Metal Catalyst	14
a. Single Electrode Measurements on Platinum, Rhodium and Iridium Black	14
b. Half Cell Measurements on Alloyed Catalysts	15
c. Comparative Full Cell Tests with Platinum and Platinum-Ruthenium Catalysts	16
3. Performance of Unsupported Platinum Metal Catalysts for Oxygen Reduction	18

4.	Thermal Stability of Unsupported Platinum Metal Catalysts	18
a.	Platinum and Rhodium Black	19
b.	Platinum Metal Alloys	19
C.	Supported Precious Metal Catalysts	20
1.	Carrier Materials for Electro-Catalysts	20
a.	Carbon	21
b.	Intermetallic Compounds and Metal Oxides	22
c.	Stability of Platinized Carbon and Carbides	23
2.	Carbon Supported Catalysts	24
a.	Physical Characteristics of Carbon Supported Catalysts	24
b.	Activity of Carbon Supported Catalysts for Methanol Oxidation	25
c.	Thermal Stability of Carbon Supported Catalysts	26
3.	Platinum Supported on Miscellaneous Substrates	29
V.	Conclusions	30
VI.	Recommendations	32
VII.	Identification of Key Technical Personnel	33
VIII.	Bibliography	34
	Appendix A - Tables	36
	Appendix B - Figures	67

LIST OF TABLES

<u>No.</u>	<u>Title</u>	<u>Page</u>
1	Surface Area of Platinum Metal Catalysts Determined by Potential Sweep Coulometry	37
2	Surface Area of Platinum Supported on Acetylene Black	38
3	Spectroanalysis of a Pt 80 Ru 20 Alloy Catalyst	39
4	Physical Characteristics of Platinum, Iridium and Rhodium Black	40
5	Physical Characteristics of Unsupported Platinum Alloy Catalysts	41
6	Methanol Oxidation on Platinum Metal Blacks	42
7	Propane Oxidation on Platinum Metal Blacks	43
8	Oxidation Potentials for Methanol on Unsupported Platinum Alloy Catalysts	44
9	Performance Data for Various Fuels on Platinum Black Catalysts	45
10	Performance Data for Various Fuels on Pt 95 Ru 5 Catalysts	46
11	Typical Composition of Anode Effluent from Propane Oxidation	47
12	Typical Composition of Anode Effluent from Ethylene and Ethane Oxidation	48
13	Comparative Performance of Unsupported Platinum Metal Catalysts for Oxygen Reduction	49
14	Thermal Aging of Unsupported Platinum Metal Catalysts	50
15	Thermal Aging of Unsupported Platinum-Ruthenium Catalysts	51
16	Characteristics of Various Prospective Carrier Materials	52
17	Stability of Platinum Activated Carbon and Selected Carbides Under Oxidizing Conditions	53
18	Crystallite Size and Bulk Density of Platinum, Iridium and Rhodium Containing Catalysts Supported on Carbon	54
19	Crystallite Size and Bulk Density of Platinum-Ruthenium Catalysts Supported on Activated Carbon	55

<u>No.</u>	<u>Title</u>	<u>Page</u>
20	Effect of Carbon Support on Physical Properties of Platinum-Ruthenium Catalysts	56
21	Methanol Oxidation on Platinum Metal Catalysts Supported on Activated Carbon	57
22	Effect of Carbon Support on Performance of Pt and Pt-Ru Catalysts	58
23	Thermal Stability of Carbon Supported Platinum Alloy Catalysts	59
24	Effect of Heating on Activity of Platinum Supported on Activated Carbon for Methanol Oxidation	60
25	Effect of Heating on Activity of Pt 35 Ru 15 C 50 on Activated Carbon for Methanol Oxidation	61
26	Effect of Heating on Physical Characteristics and Performance of Pt 40 Ru 10 C 50 Catalysts	62
27	Effect of Heating on Physical Characteristics and Performance of Pt 35 Ru 15 C 50 Catalysts	63
28	Effect of Heating on Physical Properties and Performance of Platinum-Ruthenium Catalysts Supported on Platinum Black	64
29	Effect of Heating on Physical Characteristics and Performance of Pt 35 Ru 15 Acetylene Black 50 Catalysts	65
30	Characteristics of Platinum Catalysts Supported on Miscellaneous Substrates	66

LIST OF FIGURES

<u>No.</u>	<u>Title</u>	<u>Page</u>
1	Potential Scan Coulometer	68
2	Current-Charge, Current-Voltage Curves for Unsupported Catalysts	69
3	Effect of Sweep Rates on Shape of Cathodic-Current Charge Curves	70
4	Square Wave Pulsing	71
5	Decay of Polarization for Platinum Black in Anodic Oxidation of Methanol	72
6	Polarization Decay Curve	73
7	Half Cell Arrangement for Catalyst Evaluation	74
8	Arrangement for Fuel Cell Testing	75
9	Fuel Cell Arrangement for Catalyst Evaluation	76
10	Pore Size Distribution of Pt-Black	77
11	Pore Size Distribution of an Iridium Black Catalyst	78
12	Characteristics of Pt-Ru Catalysts as Functions of Ru-Content	79
13	Pore Size Distribution of Pt(99) Ru(1) Alloy Catalyst	80
14	Pore Size Distribution of a Pt(95) Ru(5) Alloy Catalyst	81
15	Pore Size Distribution of a Pt(95) Rh(5) Alloy Catalyst	82
16	Oxidation Potentials of Methanol and Propane as Function of Ru Content in Ru Pt Catalysts	83
17	Propane Oxidation on Unsupported Pt and Pt Alloy Catalysts	84
18	Thermal Aging of Pt-Ru Catalysts	85

I. PURPOSE

The work, undertaken under this contract, consists of an investigation of fuel cell catalysts permitting complete oxidation of hydrocarbon fuels under conditions under which all reaction products are rejected from the electrolyte. Research accordingly is to be conducted to evaluate anodic catalysts and catalysts for oxygen reduction.

II. ABSTRACT

Pure and alloyed platinum metal catalysts have been investigated for the use in fuel cells operable with common hydrocarbon fuels in the temperature range from 80-200°C. The catalysts considered have adequate acid stability and considerable activity for the oxidation of carbonaceous fuels. The significance has been established of structural catalyst characteristics which determine over-all catalyst performance in addition to intrinsic factors. Catalytic activity normally increases with increasing surface area until diffusion processes in the catalyst pore structure become limiting. This is most pronounced with fuels of low electrolyte solubility but also discernible with electrolyte soluble fuels such as methanol.

Among the pure platinum metals platinum black exhibits the highest activity although its surface is smaller than that of iridium or rhodium black. Platinum black is composed of large and only loosely coherent crystallites with the surface being exposed in superficial cracks and pores which favors rapid mass transfer. Iridium and rhodium black have a high but poorly accessible internal surface.

Alloyed platinum catalysts with iridium, rhodium and ruthenium have a higher surface area than pure platinum which, however, may not always be fully usable. In contrast to platinum black these catalysts have a gel-like structure with the surface being only partially accessible. Nevertheless, alloys may markedly exceed the performance of pure platinum for anodic oxidations. In particular catalysts of the platinum ruthenium system which possess high surface areas and relatively large average pore sizes are uniquely active. Besides their intrinsic activity the superior activity of these catalysts for the oxidation of various carbonaceous fuels may be primarily attributed to these factors.

Gas chromatographic measurements showed complete oxidation to carbon dioxide of ethane, propane and butene. With ethylene, however, a small amount of carbon monoxide was also formed.

Catalysts recrystallize slowly under conditions of fuel cell operation. Since recrystallization is considerably more rapid when catalysts are heated in hydrogen rather than the electrolyte it appears likely that recrystallization occurs by a sinter process rather than by a mechanism involving dissolution of the precious metal.

Supporting the precious metal catalysts on carriers has a beneficial effect on performance due to an increase in the total metal surface area as well as a better accessibility of the active surface. In addition, improved thermal stability and catalyst life is observed. Substrates of low porosity and small particle size yield catalysts of superior activity. Thermal stability is improved, however, by the use of microporous carriers of high surface areas. Certain platinum-ruthenium alloys may nevertheless be successfully supported on carriers of low porosity to an unusual, as yet unexplained stability. Carrier materials to be considered are tantalum, tungsten or selected carbides, silicides or carbon. These substrates have adequate chemical stability at 150°C in phosphoric acid. Activated carbon and carbides are oxidized, however, at cathode potentials limiting their applicability to the fuel anode.

III. PUBLICATIONS, LECTURES, REPORTS AND CONFERENCES

Publications and Lectures

There were no publications or lectures during the period of this report.

Reports

Quarterly Reports Nos. 1 through 4 on "Fuel Cell Catalysts", Contract No. DA-36-039 AMC-03700(E).

Conferences

There were no conferences held during the period of this report.

IV. FACTUAL DATA

The work summarized in this report is a continuation of our preceding study under Contract No. DA-36-039 SC-30691 (1) concerning the characteristics and performance of precious metal based catalysts for acid fuel cells operable with economical carboreaceous fuels and air.

A. Experimental Techniques for Catalyst Evaluation

1. Physical Measurements on Catalysts

a. Determination of Surface Area, Crystallite Size and Bulk Density on Bulk Catalysts

The characterization and physical evaluation of catalysts generally involved the determination of surface area, crystallite size and bulk density using such techniques as X-ray line broadening (crystallite size) and nitrogen adsorption (total surface area BET) or carbon monoxide oxide chemisorption (surface area of active metal). These methods are known and need not be further discussed. Bulk density data given in this report were obtained by weighing a given volume of loose catalyst powder. Bulk density values indicate the particle size of the catalyst. They may be used, however, only on a comparative basis within a series of similar catalysts.

b. Measurement of Pore Size Distribution

The pore size distribution of unsupported platinum metal catalysts was determined with an Engelhard Isorpta Analyzer which employs a continuous flow method and permits pore size analysis to 600 Å and by extrapolation to 8000 Å (2). The technique involves passing a mixture of helium and nitrogen at a fixed rate and at various pressures over the sample cooled in liquid nitrogen. Nitrogen adsorbed or desorbed by increasing or decreasing pressure in the sample tube is measured continuously at near atmospheric pressure by thermal conductivity. A second gas stream, identical to that entering the sample tube, passes through the reference side of the thermal conductivity cell, thereby continuously calibrating the instrument against itself. The peak areas recorded at equilibrium adsorption can be converted to the volume of gas adsorbed per unit weight of sample. These data are related to the pore volume and pore diameter.

c. Coulometric Surface Area Determination

The anodic removal of a monolayer of hydrogen from a catalyst surface or the anodic deposition of

hydrogen starting from a bare electrode may be employed for the determination of catalyst surface areas. This electrochemical method of surface area determination, while useful for the evaluation of bulk catalysts, appears to be of particular interest in the investigation of catalysts incorporated in electrodes and the study of changes occurring during operation.

The values obtained by coulometry can differ substantially from data derived from catalyst crystallite size or gas adsorption. This is attributed to variations in the accessibility of catalyst surfaces. The surface area obtained by coulometric measurements are considered to resemble most closely the electrochemically available catalyst surface.

Potential scan coulometer: A potential scan coulometer was designed and constructed in this laboratory. The coulometer may be switched into a constant current mode of operation. A block diagram appears in Fig. 1. Potential control is obtained by placing the reference anode potential and a 0-1 volt variable calibrated potential in series with the feedback loop of a differential amplifier. The output of the control amplifier (0-20 mA) is fed into a current amplifier consisting of four transistors in complementary symmetry (class B) operation. Output is 5 volts, ± 1 amp maximum. Two other operational amplifiers are connected as integrators by the use of low leakage capacitors, one generates a potential ramp (0-2 volts) of variable slope (0.05-500 volts/sec.) by integration of a constant potential and the other integrates a fraction of the cell current between potential limits determined by a dual coil relay of 1 millisecond operating time powered from the sweep amplifier. The charge passed is read out as a voltage and the integrator calibrated by integration of a constant current for a known time. Potential is measured between the hydrogen reference electrode and the anode by a digital voltmeter and the current by a shunted 100-0-100 microammeter or, alternatively, the potential observed across a calibrated series resistor. The three differential amplifiers are P45, G. A. Philbrick Researchers Inc. analogue computer solid state devices. The instrument is battery powered throughout.

Anodic potential scans: The surface areas of representative catalyst samples were determined by the anodic removal of hydrogen by a linear potential sweep in the range from 0 to 1600 mV. Measurements were carried out with teflon bonded catalyst samples

at 25°C in 2 N sulfuric acid using a half cell as described on pp. 9-10. The following procedure was employed: The electrode potential was set at the hydrogen potential for 10 minutes, during which time a high cathodic charge passed, to fully reduce the catalyst. The potential was then set at +20 mV versus hydrogen for 5 minutes and an anodic sweep up to 500 mV imposed at the rate of 0.05 V/sec. The electrolyte was vigorously purged with purified nitrogen during these operations. A plot of current versus charge was made using an X-Y plotter (Electronic Associates Inc., "Variplotter" Model 1100E). The curves were reproducible after a wait time of 2 minutes and were independent of the nitrogen stirring rate. The charge passed at the current minimum was recorded and the electrode potential set at +25 mV for five minutes. The process was then repeated for increments of +5 mV starting potential up to +80 mV.

The charge passed at the current minimum decreased with increase of starting potential due to a reduction in the current caused by extraneous hydrogen. At about +55 mV starting potential the charge passed was assumed to correspond only to adsorbed hydrogen removal. A series of current-charge curves for the case 5% Ir 95% Pt appear in Fig. 2 (a). It can be seen that the charge passed at the current minimum becomes independent of starting potential for starting potentials in the range +55 \longleftrightarrow +65 mV.

The current voltage scan in the case of platinum black appears in Fig. 2 (b), there is a well defined minimum of current at about 10% of peak. Iridium 5, platinum 95, and rhodium 5 platinum 95 scans have essentially the same shape. For ruthenium 5 platinum 95, however, the minimum is at about 40% of peak, and ruthenium 30 platinum 70 does not exhibit a minimum. This effect may well be caused by the formation of a chemically held oxygen film on the catalyst, starting at low potentials and promoted by the ruthenium, since removal of this film can only slowly be achieved. This effect vitiates the measurement of surface area by this method.

Surface areas are calculated from the charge required to remove adsorbed hydrogen assumed to exist as a monolayer of one hydrogen atom per platinum atom and using the calculated figure 0.21 millicoulombs of charge for hydrogen removal per unit of real area of platinum (3). The same value was used for calculating surface areas of platinum alloys. In the value the charge provided by the necessity of changing the potential of the double layer is not taken into

consideration. In the case of platinum or platinum alloys having platinum as their major constituent this may involve an error of not more than 5%. Assuming a maximum double layer capacity of $20 \mu\text{F}/\text{cm}^2$ the charge contributed by the charging of the double layer is 10^{-5} coul. for a 500 mV potential change compared to 2×10^{-4} coul. for adsorbed hydrogen removal.

Cathodic potential scan coulometry: The cathodic deposition of hydrogen starting from a presumably bare electrode was investigated as an alternative method for the determination of catalyst surfaces. The current-coulomb graphs obtained in 2 N sulfuric acid at 25°C are shown in Fig. 3 for platinum black at various sweep rates starting from a potential of 500 mV vs. hydrogen. Distinct current minimas are only obtained at slow sweep rates ≤ 0.05 volts/sec. The charge passed was independent from starting potentials between +350 mV to 650 mV. The surface area was calculated from the charge passed between point B and A on the graphs shown in Fig. 3. Values as shown in Table 1 are obtained for Pt and Rh black and alloys of Pt-Ir or Pt-Rh assuming one hydrogen atom per metal atom. The surface area data obtained by anodic coulometry are also summarized in Table 1 and compared to values obtained by other methods.

The surface area as measured by anodic or cathodic potential sweep coulometry is in excellent agreement with gas adsorption data in the case of platinum. Lower values are obtained for alloyed samples, particularly by cathodic coulometry. This is attributed to the poorer accessibility of the surface (micro pore structure) in these cases.

Carbon supported catalysts: The applicability of cathodic potential sweep coulometry was also investigated in the case of platinum supported on acetylene black (metal concentration 50% by weight).

The values obtained by cathodic coulometry as well as carbon monoxide chemisorption and calculation from crystallite size are summarized in Table 2. Also included are surface areas of samples which had been altered by heat treatment in hydrogen at 120°C and 200°C . The Table also shows BET data indicating the total platinum and carbon surface of the catalysts. The agreement is closest between calculated data and values obtained by chemisorption, whereas a considerably higher surface area is obtained by cathodic coulometry. The discrepancy increases in fact with heat treatment of the catalyst. Since unplatinized acetylene black is

inactive under these conditions, it appears that atomic hydrogen is diffusing from platinum sites onto the carbon carrier thus increasing the total charge needed to complete the hydrogen monolayer. Surface diffusion of hydrogen on platinum activated carbon has recently been investigated (4). A free mobility of hydrogen from platinum onto carbon sites surrounding platinum centers has been suggested by these experiments.

2. Electrochemical Evaluation of Catalysts

a. Catalyst Evaluation by Transient Techniques

The determination of catalyst activity under conditions eliminating the limitations imposed by mass transfer in the electrode and catalyst structure appears to be desirable for a better understanding of the factors governing catalyst performance and may serve as a guide in the development of improved preparations.

Chemical and electrochemical methods have been described in the literature for the purpose of catalyst testing. The hydrogen deuterium exchange reaction for fuels adsorbed on the catalyst surface has been explored by studying the catalysts for the electro-oxidation of hydrocarbons (5,6). An attempt has also been made to relate fuel cell activity to the quantity of adsorbed fuel, in this case methanol at open circuit (7). For the oxidation of formic acid the correlation between catalytic activity and the free surface present under load have been studied (8). A variety of techniques are under investigation to determine the role of adsorption processes in the electrochemical oxidation of fuels (9).

We have carried out an examination of the applicability of relaxation methods for catalyst evaluation. The possibility of separating activation and diffusion controlled electrode polarization by means of differences in the decay of electrode polarization with time has been investigated. In the literature, the relaxation of electrode polarization has been described and a theory applicable for fuel concentration polarization under small displacement of the system from equilibrium has been developed (10).

Experiments: The relaxation of electrode polarization has been investigated in the case of methanol in 2 N sulfuric acid at 90°C. Under these conditions the electrode polarization is independent of methanol concentration at the usual fuel concentration of .5 mol/l

employed and it is, therefore, electrolyte transport and activation polarization which contribute to the over-all polarization observed (11).

Current pulses from a repeat cycle timer (Wilson Co. Model No. 3) were applied to an electrode of teflon bonded platinum black (1:1) and the potential time trace was displayed on an oscilloscope externally synchronized from the timer. The traces were photographed. A circuit diagram appears in Fig. 4 and typical shapes of the potential time traces are shown in Figs. 5a and 5b.

Fig. 5a illustrates the response to an equal off-on time current square wave of 100 mA/cm² height; decay curves are smooth over the range used (≈ 200 mV decay and recovery).

Fig. 5b shows a decay curve over about 350 milliseconds after an imposed square wave of 100 mA/cm² height lasting 30 milliseconds.

A series of single shot decay curves covering a time scale of 10 milliseconds to 10 seconds were photographed and a curve of $\Delta\eta$ ($=\eta_0 - \eta_t$) plotted against $\log t$ in Fig. 6, where η_0 is the polarization at $t = 0$, i.e. the steady state polarization prevailing before current interruption, and η_t is the polarization at time t after current interruption. Therefore, $\Delta\eta$ is a positive quantity equal to the amount of potential recovery from steady state polarization in time t .

The graph has a slope of approximately 100 mV/decade of time. No real change in slope is evident within experimental error. Thus, separation of the two major types of polarization does not appear feasible at least in the time range investigated. Presumably, an interdependence of transport and activation controlled electrode processes exists and both types of polarization may decay at comparable rates.

b. Current-Potential Measurements

The electrochemical activity of catalyst was determined essentially by current-potential measurements at moderate or high current densities. No studies in the Tafel region were undertaken; the value of such measurements appears to be limited in the case of high surface area catalysts.

Half cell testing: Most performance data given in this report were obtained at essentially atmospheric pressure on single electrodes. The catalyst was incorporated for the purpose of evaluation into an electrode structure

by the following procedure: Sieved samples of catalyst (-400 mesh) were mixed with teflon powder (-50 mesh). The mixture containing from 20% to 60% of teflon was pressed in a thin layer onto an 80 mesh platinum screen, usually at a pressure of 1000 lbs./sq. inch. The stability of these electrodes was adequate for testing over periods of several hours. The polarization data obtained with these test electrodes may only be viewed as a characterization of catalyst activity on a comparative basis since, undoubtedly, diffusion limitations in the structure are somewhat varying and, therefore, contribute in a varying yet significant degree to the total overvoltage observed. Nevertheless, this does not materially affect the rating of catalyst.

The half cell used for current potential measurements at elevated temperatures is shown in Fig. 7. The cell is heated by an oil bath and provided with a reflux condenser to maintain constant acid concentration. Potentials were measured by means of a hydrogen electrode incorporated in a Luggin capillary as shown in Fig. 7. The reference electrode operates at the same temperature and in the same acid as the test electrode, thus uncertainties due to diffusion potentials are eliminated.

The reference electrode consisting of a platinized screen is maintained at essentially the hydrogen potential by passing a small cathodic current. This type of reference electrode is practically identical with that described recently by Giner (12).

Full cell arrangement for catalyst evaluation: For evaluation of catalysts and the study of electrode processes under actual operating conditions a full cell was built operable under controlled humidity up to temperatures of 200°C. A schematic diagram of the cell arrangement appears in Fig. 8.

The cell and the fuel gases are brought to operating temperatures in a chamber heated by strip heaters attached to the walls. A uniform temperature and a rapid heat transfer is obtained by a fan. The fuel gases as well as air or oxygen may enter the system through separately heated humidifiers mounted on the outside of the oven or may enter the cell dry by means of a by-path.

Cell design: A more detailed description of the cell employed is given in Fig. 9. A sandwich type cell construction using a trapped phosphoric acid electrolyte system is employed. The catalyst is directly imbedded

into the membrane containing the electrolyte and the current is collected by means of a fine and a coarse platinum screen. The latter also provides a path for the fuel gases.

The entire cell assembly is held between teflon and steel plates. Potential readings are taken by means of two hydrogen reference electrodes which are inserted into the teflon plates and contact the test electrodes by an electrolytic bridge. Auxiliary electrodes are used to maintain the reference electrodes at the hydrogen potential.

Chromatographic analysis of cell effluent: As indicated in Fig. 8 a chromatograph was directly connected to the fuel cell. The sample of the anode effluent was admitted to the instrument after the water was condensed in a cold trap (ice) and a magnesium perchlorate drier. A F & M Chromatograph Model 700 with a micro cross section detector was employed.

Good results were obtained with a 25 ft. silica gel column and hydrogen as carrier gas with a flow rate of 110 cc/min. The temperature of the column was kept constant at 55°C and that of the detector block at 120°C. The decrease in radio activity was frequently checked by a calibration test mixture and was taken into account for the evaluation of the chromatograms. For greater sensitivity a flame detector cell and dimethyl sulfolane on chromosorb or silica gel as column material was also employed.

B. Unsupported Platinum Metal Catalysts

The properties and performance of catalytic blacks of platinum, rhodium, iridium and of alloys of platinum with ruthenium, rhodium and iridium are discussed. These catalysts warrant investigation since they are characterized by electrocatalytic activity as well as by good chemical stability. They form solid solutions over a wide range of concentrations.

The activity of the pure platinum metals and alloys was investigated for both the reduction of oxygen and the anodic oxidation of representative fuels in phosphoric and sulfuric acid electrolytes. Catalysts discussed in this section were obtained in the form of finely divided blacks by chemical reduction methods. The preparation techniques employed yield catalysts with low impurity content as evident from Table 3 showing the spectroanalysis for a representative platinum-

ruthenium sample (platinum/ruthenium ratio approximately 4:1). Typically, these catalysts contain about 99.5% of the platinum metal or platinum metal alloy, the major impurity being palladium. In addition to palladium, some iridium, aluminum and boron are present as other noticeable contaminants.

1. Physical Properties of
Unsupported Platinum Metal Blacks

a. Pure Metal Blacks

A number of high surface area iridium and rhodium blacks were prepared and compared to commercial Engelhard platinum black. Typical data of the surface areas, crystallite sizes and bulk densities of these catalysts appear in Table 4. In Figs. 10 and 11 the pore size distribution is illustrated.

A considerably higher surface area and smaller crystallite size is evident for rhodium and especially iridium black than observed with Pt black. Both metals, however, have a higher bulk density than platinum (with reference to true density) which is indicative of large catalyst grains. In view of the large surface area a micro-porous gel-like catalyst must be assumed. This conclusion is supported by the differences observed between surface area values obtained by electrochemical or BET measurements. Obviously the catalyst is only partly accessible to gas as well as electrolyte, particularly in the case of iridium.

Major differences in the pore structure of the catalysts are also apparent. In the case of platinum a maximum in the pore volume may be noted in the 10-15 Å range decreasing slowly with increasing pore diameter. These pores, presumably, represent surface roughness and surface cracks in large and only loosely agglomerated platinum crystallites.

The pore structure of iridium black is shown in Fig. 11. Two distinct maxima in the 20 Å and 40 Å range are discernible indicating two different types of pores which could be attributed to a gel-like catalyst structure, the larger pores being made up by holes in the gel whereas the smaller pores may represent the pore structure in the crystal agglomerates. The significance of these data for the performance of the blacks as anode catalysts is discussed in Sections B.2.a, 2.b.

b. Alloy Blacks of Platinum with Ruthenium, Rhodium and Iridium

Representative crystallite size, surface area and bulk density data for alloy blacks are shown in Fig. 12 and Table 5. The pore size distribution of selected samples is illustrated in Figs. 13-15.

Alloying platinum markedly affects catalyst crystallite size, surface area and bulk density. With additions of 5% ruthenium, crystallite size is roughly halved as compared to platinum black. Iridium and rhodium appear to be equally effective based on the same molar concentrations.

In the case of platinum-ruthenium alloys the decrease in crystallite size is most rapid up to concentrations of 10% ruthenium with further additions only resulting in a gradual decrease.

In agreement with the smaller crystallite size a substantially higher surface area is observed with alloyed catalysts. Thus preparations containing 5% ruthenium have a surface area as measured by nitrogen adsorption approximately twice that of platinum black. At ruthenium contents of 20-30% a surface area of 80-90 m²/g or 3-4 times that of platinum black is obtained.

However, with alloying the grain sizes increase rapidly above those of platinum black as evident from bulk density data in Table 5 and Fig. 12 used as a qualitative description of grain size. In all cases a substantial increase is obtained by alloying. For instance, bulk density of a 30% ruthenium catalyst is 2.4 g/cm³ as compared to .55 g/cm³ of platinum black.

Comparison of surface area data: The surface area of catalysts as shown in Table 5 was calculated from crystallite size or measured by gas adsorption, respectively, or by electrochemical techniques described in section A.1.c., pages 4-8.

Considerable differences in catalyst surface area were observed depending on the method employed.

The lowest data were obtained by the electrochemical method, followed by gas adsorption. Remarkably higher values resulted on the other hand from calculations based on crystallite size. The differences vary widely with the catalyst. Thus with platinum a relatively good agreement is observed between the electrochemical method and gas adsorption, whereas the value calculated from crystallite size data is about 20% higher.

For a catalyst containing 5% ruthenium and 95% platinum a surface area of 40 m²/g is obtained electrochemically, whereas 48 m²/g are measured by gas adsorption. The corresponding calculated figure is 66 m²/g.

The variations observed between the methods are attributed primarily to the difference in the accessibility of the surface area. The coulometric surface determination yields the lowest values, these data however represent best, it appears, the actually usable catalyst surface.

Pore size distribution of alloy catalysts: The pore size distribution of platinum alloy catalysts with ruthenium contents of 1% and 5% is illustrated in Figs. 13 and 14. Both catalysts have a complex pore structure. A considerable fraction of the total pore volume is present in pores over 100 Å and compared to platinum a greater average pore diameter is evident increasing with greater ruthenium content.

Obviously, this open pore structure of ruthenium-platinum catalysts is one of the reasons for their superior activity observed for the anodic oxidation of a variety of organic molecules (13).

The pore size distribution of a platinum catalyst containing 5% rhodium is shown in Fig. 15. The pore structure of this catalyst is similar to platinum black. The major pore volume is present in pores of approximately 20 Å. A second peak occurs, which is not noticeable with platinum, at 40-50 Å possibly indicating a loose grouping of crystal agglomerates of the alloy.

2. Anodic Performance of Unsupported Platinum Metal Catalyst

The data contained in this report are primarily concerned with correlations between the physical characteristics of catalyst systems such as described in section B.1. and their anodic performance. It should be pointed out that the experimental data were only comparative within a given series of tests.

a. Single Electrode Measurements on Platinum, Rhodium and Iridium Black

The electrochemical activity of unsupported catalysts was tested in half cells as discussed in section A.2.b. Polarization curves were determined for methanol and propane oxidation in sulfuric acid or phosphoric acid electrolyte.

Unsupported platinum, rhodium and iridium blacks:
Pertinent test results for methanol and propane oxidation on platinum, rhodium and iridium blacks are shown in Table 6 and Table 7. In contrast to earlier findings (14) the highest activity for methanol oxidation is observed with iridium followed by platinum and rhodium. The differences are particularly marked at lower current densities whereas at higher current drains iridium performs only slightly better than platinum. Presumably, the relatively large grain size of iridium black is a limiting factor even with an electrolyte soluble fuel such as methanol.

For the oxidation of propane platinum is a superior catalyst and neither iridium nor rhodium show any significant activity. Again, in the case of iridium and to a lesser degree rhodium the larger grain size, undoubtedly, is one reason for the lack of activity. Considering the high surface area of iridium a lower intrinsic activity may also be responsible. These findings are in agreement with recent studies concerning the electrooxidation of ethylene on platinum metals. A decline in activity in the order platinum, rhodium, iridium was found for this fuel (15).

b. Half Cell Measurements on Alloyed Catalysts

Platinum-ruthenium system: Polarization data for methanol at 95°C in 2 N sulfuric acid and for propane at 150°C in 85% phosphoric acid are illustrated in Fig. 16 as a function of ruthenium content in the platinum-ruthenium alloy catalysts. Readings were taken after several minutes of current drain at a current density of 50 mA/cm² and at a catalyst loading of 50 mg/cm².

Activity for methanol oxidation: Oxidation potentials for methanol decrease from .45 volts for platinum black to .29 volts vs. hydrogen in the same solution for a catalyst with 20% ruthenium. A further increase in ruthenium concentration does not improve performance. The increase in activity with addition of ruthenium is in line with the surface areas and crystallite sizes of ruthenium-containing catalysts shown in Fig. 12. It may be noted, however, that polarization decreases only slightly once 10% ruthenium has been added, whereas a further increase in ruthenium content still markedly changes crystallite size and surface area.

Activity for propane oxidation: The activity of platinum for the oxidation of propane also improves by alloying with ruthenium. Contrary to methanol,

however, a pronounced optimum in performance is observed with catalysts containing only 5% ruthenium. Activity decreases rapidly at higher concentrations.

In interpreting these results it appears that the differences in the performance of platinum-ruthenium catalysts for methanol and propane oxidations are essentially due to fuel and mass transfer limitations in the microporous catalyst structure. As stated before, relatively large catalyst grains are formed at higher ruthenium concentrations with the surface area largely available in micropores. Obviously, with propane being only slightly electrolyte-soluble a major fraction of this area may not be used for the electrochemical reaction, explaining possibly the performance decline with this fuel at concentrations above 5%. With methanol such limitations appear to be apparent at a content over 10% ruthenium.

Platinum alloys with iridium and rhodium: Oxidation potentials for methanol and propane on catalysts containing 95% platinum and 5% of either iridium and rhodium are shown in Fig. 17 and Table 8. For comparison the performance of platinum black and platinum alloyed with 5% ruthenium is illustrated. Tests were carried out in 85% phosphoric acid at 150°C. The data show performance as obtained after several minutes of current drain. A correlation exists between activity and catalyst surface area. The over-all activity for propane oxidation improves simultaneously with surface in the sequence: platinum, platinum-iridium, platinum-rhodium, platinum-ruthenium. However, there seem to be differences also in intrinsic activity. For instance, the relatively poor performance of platinum-rhodium catalysts constitutes a deviation from the surface correlation observed with propane.

c. Comparative Full Cell Tests with
Platinum and Platinum-Ruthenium Catalysts

A series of comparative tests have been carried out in the full cell described on page 10 using platinum or platinum 95 ruthenium 5 as anode catalysts. Platinum black was employed exclusively on the cathode. The reactivity of a variety of fuels was evaluated and a complete chromatographic analysis of the anode effluent was undertaken.

A summary of the test data appears in Tables 9-10. The data may be considered representative of cell operation at least for several hours. The cells have been operated continuously up to 300 hours in this testing program. The data given are actual cell

voltages from which the anode potentials can be derived by deducting the cell voltage from the output observed with hydrogen. (Polarization of the anode with hydrogen is below 10 mV at 100 mA/cm² and may be neglected.) Below follows a description of the tests and a discussion of the observations made. The analysis of the cell effluent was carried out as described on page 11.

Cell Operation: The design and operating principles of the full cell employed have briefly been discussed in section A.2.b., pages 10,11. The following details may be added at this point: Newly assembled cells were first operated for one day with technical grade hydrogen. In this period normally a steady cell performance was reached with the output from various cells reproducible to ± 10 mV at 100 mA/cm².

Contrary to carbonaceous fuels hydrogen was admitted dry to the cell; an undetermined yet very small excess of fuel was employed. Technical grade oxygen was passed through the cathode compartment in excess (5-15 ml) removing the water generated. Typically 1-2% of oxygen were found in the anode effluent which presumably entered the anode compartment through leaks in the edge-gaskets of the cell. This leakage was found not to affect cell performance. Diffusion of oxygen through the electrolyte must have been insignificant since the anode potentials observed were in good agreement with those measured on single electrodes.

Ethane, propane, butane: The reactivity of these fuels is equal within the limits of experimental error. The platinum-ruthenium alloy exhibits a considerably higher activity than platinum black. In all cases humidification was required to maintain electrode activity. The fuel gases were saturated at 83-86°C; the optimum degree of humidification was not determined. Performance data shown in Tables 9 and 10 were obtained at a gas flow corresponding to a fuel conversion ranging from 5-10%. In general, cell performance was steady at higher loads while a slow decline did occur at lower current drains. Possibly more positive anode potentials at higher loads accelerate the oxidation of intermediates or side products adsorbed on the catalyst which may accumulate otherwise.

The chromatographic analysis of the anode effluent for propane and ethane oxidation is summarized in Tables 11 and 12. Using propane as fuel carbon dioxide was found to be the only reaction product on both catalysts. The current density was 50 mA/cm² and the flow rate

corresponded to a 5% fuel conversion. Some ethane present as impurity in the propane feed was consumed to a similar extent as propane. Methane which was also present in the feed gas was not affected. A change in current density from 50 mA/cm² to 105 mA/cm² keeping the other variables constant only resulted in a higher fuel conversion and, accordingly, increased carbon dioxide content (27%) in the effluent. At open circuit (propane) only .2% carbon dioxide was observed in the anode effluent formed presumably by chemical combustion with oxygen diffusing into the anode compartment.

In the case of ethane, again, the major reaction product was carbon dioxide. A small quantity of ethylene which was present in the feed gas was selectively removed after contacting the anode. Possibly, ethylene which is more strongly chemisorbed is preferably oxidized. Hydrogenation of ethylene to ethane, however, may also not be ruled out.

Ethylene and carbon monoxide: Contrary to earlier findings (16) Pt-Ru catalysts did exhibit a higher activity than platinum black for the oxidation of carbon monoxide. As with hydrocarbons, however, humidification was required. The reactivity of both ethylene and carbon monoxide, fuels which are strongly chemisorbed, is considerably below that of ethane, propane and butane. Ethylene was the only fuel where some carbon monoxide was found as reaction product although in traces only.

3. Performance of Unsupported Platinum Metal Catalysts for Oxygen Reduction

The activity of unsupported blacks of platinum, iridium and rhodium as well as alloys of platinum with small quantities of ruthenium, iridium and rhodium was tested for oxygen conversion. Tests were carried out in 7.5 N sulfuric acid at 80°C and atmospheric pressure in a half cell. Pertinent test data are summarized in Table 13. Within limits of experimental error none of the catalysts tested exceeded the performance of platinum black. Iridium and rhodium exhibited substantially lower activity than platinum black in spite of a much higher surface area. Among the alloyed catalysts, platinum containing 1% ruthenium has an activity comparable to platinum black. Alloys with 5% ruthenium, iridium or rhodium are again markedly inferior.

4. Thermal Stability of Unsupported Platinum Metal Catalysts

Platinum metal catalysts obtained in high surface area form by low temperature reduction methods are known to recrystallize at elevated temperatures (17). In the case of platinum

black, for instance, sintering has been observed at temperatures above 100°C (18). Undoubtedly, under conditions of fuel cell operation recrystallization of the catalyst does occur and is one of the major reasons for the permanent decline in electrode performance.

Aging of unsupported catalysts was investigated at 120°C in an atmosphere of hydrogen. Catalysts were heated for a two hour period and changes in crystallite size, surface area and bulk density determined.

This treatment is indicative of the over-all stability of a catalyst and has been employed to obtain such data. The aging at the same temperature of an operating catalyst in contact with electrolyte may be different and is expected to be usually less drastic.

The recrystallization of unsupported platinum metal catalysts is particularly rapid in a hydrogen atmosphere, presumably by providing a clean metal surface. Similar observations have been made elsewhere (19).

a. Platinum and Rhodium Black

The effect of heating in hydrogen on crystallite size, surface area, and bulk density is shown in Table 8 for platinum and rhodium black. As a result of heating, a considerable recrystallization accompanied by a decrease in surface area and increase in bulk density occurs. Compared to platinum, rhodium black appears to have a superior stability.

b. Platinum Metal Alloys

Alloys of platinum with iridium and rhodium: The stability of platinum alloys with 5% additions of either iridium or rhodium is also shown in Table 14. Again, a marked increase in crystallite size may be noted accompanied by a loss in surface area. The increase in bulk density is considerably greater than that observed with the pure metal blacks.

The heating of catalysts in hydrogen does result in some loss in catalytic activity which is lower, however, than to be expected from the decline in surface area. In the case of platinum 95 iridium 5, for instance, the surface area decreased from 38 m²/g to 19 m²/g, whereas oxidation potentials for propane measured at 150°C and at a current density of 100 mA/cm² increased only from .36 volts vs. hydrogen to .39 volts.

Presumably, as a result of recrystallization the major loss in surface area occurs in small pores which contribute little to the catalytic activity.

Platinum-ruthenium system: Surface area, crystallite size and bulk density of heated ruthenium-platinum alloy catalysts with ruthenium concentrations ranging from 1-30% are shown in Fig. 18 and Table 15. A substantial increase in crystallite size and bulk density may be noted as a result of heating, accompanied by a drastic drop in surface area as measured by the BET method. As to be expected, the stability decreases with increasing surface area, that is, higher ruthenium content. Thus, with a catalyst containing 5% ruthenium a decline in surface area to about 40% of the original value is observed, whereas a catalyst containing 40% ruthenium lost roughly 80%. It is interesting to note that changes in surface area are not substantiated by an equivalent increase in crystallite size, particularly at higher ruthenium concentrations. Thus the observed loss in surface area must be partly attributed to a lesser accessibility of the catalyst surface.

The catalyst recrystallization is not as pronounced under actual operating conditions. The above mentioned catalyst containing 5% ruthenium was tested at 150°C in phosphoric acid employing propane as fuel. The crystallite size increased from 52 Å to 64 Å in a 24 hour period as compared to an increase to 83 Å observed after heating for two hours in hydrogen. A platinum black sample having a crystallite size of 86 Å and a surface area of 28 m²/g showed an increase to 122 Å under the same conditions. These findings are in agreement with the better life performance of platinum-ruthenium catalyst as compared to platinum which was demonstrated earlier (20).

C. Supported Precious Metal Catalysts

In this section the characteristics are discussed of carrier materials and the physical properties and electrochemical activity of carbon supported iridium, platinum and rhodium as well as platinum alloys with iridium, rhodium and ruthenium. The support of precious metal catalysts on suitable carriers is considered to be of significant importance in the development of effective electro-catalysts. Carriers may permit a dilution of the precious metal component either by a decrease in the crystallite size or a decrease in the size of the precious metal grains whereby additional internal surface is exposed. Supporting structures are also known to contribute to the thermal stability of platinum metal catalysts (17).

1. Carrier Materials for Electro-Catalysts

A survey of prospective carrier materials for the support of fuel cell catalysts operable in concentrated phosphoric or sulfuric acid

electrolytes has been undertaken. This study involved an evaluation of several carbon materials and a preliminary screening of certain carbides, silicides, borides and oxides with promising chemical stability (21). Also included in this study were tungsten and tantalum powders.

a. Carbon

Carbon carriers have been widely used for the support of low temperature fuel cell catalysts either in the form of finely divided powders (22) or as supporting porous structures. Carbon has been reported to be inert to chemical corrosion in phosphoric acid at 150°C, also no attack was observed up to potentials of 1 volt (23). The structure and physical properties of some commercially available carbon carriers are illustrated in Figs. 19, 20.

Two samples, namely Ling Temco Vought 230 and Ling Temco Vought 239* have a low surface area of less than 20 m²/g while the particle size as indicated by the bulk density is high. LTV 239 is a carrier of very low porosity, a small maximum of the pore volume may be noted at a diameter of 22 Å. LTV 230 has a higher porosity and a pronounced maximum in pore volume at 16 Å pore diameter.

Acetylene black, another carrier investigated is characterized by a very low bulk density and a moderately high surface area and porosity. It is interesting to note that the pore volume is to a large extent in pores over 50 Å diameter, whereas no micropores of less than 20 Å diameter are noticeable.

Activated carbon possesses a high surface area with about ten times the porosity than that of acetylene black.

Structure and physical properties of the carrier have a pronounced effect on performance and stability of electro-catalysts which is discussed on pages 25, 26.

* We want to express our appreciation to Dr. M. W. Reed of Ling Temco Vought Co. for supplying these carbon materials.

b. Intermetallic Compounds and Metal Oxides

Most carrier materials generally employed for the support of catalysts are of insufficient stability towards concentrated acids to be of utility for the preparation of electro-catalysts and new substrates must be developed. We have studied the physical characteristics and possible utility of tantalum, tungsten and of certain silicides, carbides, borides and oxides which were selected on the basis of reported acid stability (24). The properties of commercially available powders are listed in Table 16. The surface area of most samples is insufficient for the support of catalysts. Possibly, a further increase could be obtained by etching.

Electrical resistance: Electrical resistance data given are either literature values pertaining to massive specimen or measured values applying to powders compacted at a pressure of 5000 lbs./sq.inch. The considerable difference between these values illustrate the effect of high resistance surface layers (oxide) which appear to be present in most cases.

Chemical stability: The stability of the materials listed in Table 16 was tested in 85% phosphoric acid at 150°C. Usually, 2 g samples of the powders were heated in 50 ccm of acid for a period of two days while air was bubbled through the solution. The acid concentration was maintained by a reflux condenser. The powders were weighed afterwards and examined for changes in appearance while the solutions were analyzed. Based on this evaluation the following materials were excluded from any further study: Chromium boride, zirconium disilicide, titanium disilicide, chromium carbide, molybdenum disilicide and silicon carbide. With the exception of molybdenum disilicide and silicon carbide, which were only slightly attacked, the samples were either dissolved, decomposed or both in phosphoric acid.

Metallic tantalum and tungsten, tantalum disilicide, tantalum oxide and tungsten oxide showed no apparent change. Stability was further exhibited by boron carbide and tungsten carbide.

c. Stability of Platinized Carbon and Carbides

The stability of platinized samples of carbon, boron carbide, silicon carbide and tungsten carbide was investigated at temperatures ranging from 100-200°C in the matrix cell described on page 10. Catalysts containing 50% by weight platinum were employed. They were incorporated into test electrodes with a total geometric surface area of 20 cm² by bonding with teflon (25% by weight).

Stability of platinized carbon at anodic potentials: Little information has become available as yet concerning the stability of platinum-activated carbons in acid electrolytes at elevated temperatures at potentials of fuel anode operation. Oxidation of platinized carbons has been observed, however, at cathodic potentials in sulfuric acid (24).

A potential of .3 to .5 volts vs. hydrogen was imposed on the anode with a potentiostat while anode and cathode compartments were purged with humid nitrogen (partial pressure of water approximately 400 mm Hg) at a rate of 15 cm³/minute. At temperatures ranging from 100°C to 200°C no carbon dioxide was detected by infrared analysis (Perkin Elmer Model, detection limit for carbon dioxide is 60 ppm) in the effluent gases, indicating stability of carbon in this potential range.

In the presence of oxygen in the cathode compartment, however, considerable oxidation occurred in the above mentioned potential range on the anode. A carbon dioxide content of 200-250 ppm was observed independent of temperature, which is primarily attributed to chemical oxidation of carbon by oxygen diffusing into the anode compartment.

Stability of platinized carbon and carbides at cathodic potentials: The carbon dioxide content of the cathode effluent for platinum activated acetylene black, boron carbide, and silicon carbide is illustrated in Table 17. Rapid oxidation of carbon occurred at temperatures between 100°C and 150°C, particularly at open circuit when oxygen was fed to the cathode compartment. No improved stability was exhibited by boron carbide, silicon carbide and tungsten carbide in this temperature range.

2. Carbon Supported Catalysts

a. Physical Characteristics of Carbon Supported Catalysts

Pure platinum metals and alloys of platinum with iridium, rhodium and ruthenium were supported in concentrations ranging from 25-75% by weight on representative carbon carriers discussed on page 21. Crystallite size and bulk density of catalysts were determined.

Carbon supported catalysts containing platinum, iridium, rhodium: Typical crystallite size and bulk density data for catalysts supported on activated carbon and acetylene black in a concentration of 50% are summarized in Table 18. For comparison data for unsupported catalysts are also listed. The catalyst crystallite size is markedly reduced as a result of the carrier only in the case of platinum. No change is observed in the case of iridium.

Crystallite size data for carbon supported catalysts should be viewed as being qualitative only because the determination of crystallite size on supported catalysts by X-ray diffraction methods may involve a considerable error, particularly in the range below 20 Å.

Carbon supported platinum-ruthenium catalysts: Crystallite size and bulk density data for platinum-ruthenium alloy supported on activated carbon, acetylene black and Ling Temco Vought carbons are summarized in Tables 19 and 20.

The widely varying surface area and pore structure of the carbon carriers employed has a considerable effect on crystallite size and bulk density. The highest crystallite size (smallest platinum area) is obtained on low surface area Ling Temco Vought carbons.

A substantial decrease of crystallite size takes place as the surface area of the support is increased by the use of acetylene black or activated carbon. It is interesting to note, however, that both acetylene black and activated carbon yield catalysts of comparable crystallite

size in spite of a great difference in surface area of the carrier. Compared to unsupported blacks only preparations on activated carbon or acetylene black exhibit a lower crystallite size.

The bulk density of the catalyst depends to a great extent on the carrier material. The lowest density powders are obtained with acetylene black as support. Usually, platinum-ruthenium alloys exhibit a higher bulk density than carbon supported platinum which is attributed to some agglomeration.

b. Activity of Carbon Supported Catalysts for Methanol Oxidation

Oxidation potentials for methanol were determined in 2 N sulfuric acid at 90°C and in 85% phosphoric acid at 140-150°C.

Performance in phosphoric acid: Test data at 140-150°C (in phosphoric acid) are summarized in Table 21. Among the catalysts evaluated the ruthenium alloy shows the highest activity followed by platinum-rhodium. With ruthenium alloy catalyst limiting currents of approximately 200 mA/cm² were observed with precious metal loadings of 9 mg/cm². At a current density of 100 mA/cm² potentials of about 200 mV versus hydrogen in the same electrolyte were measured. This compares with a polarization of 30 mV using hydrogen instead of methanol fuel under the same conditions.

The catalysts tested in phosphoric acid were all supported on activated carbon. Although the pore structure of this carrier material is not particularly favorable, much lower catalyst loadings may be employed than with unsupported samples without detrimental effect on electrode activity.

The relative performance of supported catalysts is, however, not always consistent with the activity of unsupported blacks. Thus, the activity of platinum on carbon marginally exceeds the performance of supported iridium, contrary to findings with pure platinum and iridium black (Table 6).

Performance in 2 N sulfuric acid: A comparison of activity of platinum-ruthenium catalysts (70% platinum, 30% ruthenium on a metal basis) supported on activated carbon, acetylene black and Ling Temco Vought appears in Table 22. These data illustrate in particular the effect of pore structure, bulk density and surface area of the carrier on catalyst performance for the oxidation of an electrolyte soluble fuel such as methanol.

At high current densities, e.g. 200 mA/cm², a comparable performance of activated carbon and Ling Temco Vought 239 supported catalysts is observed, although the crystallite size of the active metal is considerably higher on the LTV 239 support (Table 20). Possibly, the higher crystallite size is compensated by a better accessibility of the catalyst surface on this essentially non-porous carrier. The sample supported on LTV 230 exhibits lower activity which may be related to its higher porosity and microporous structure (Fig. 20).

The best activity at high current densities is obtained with catalysts supported on acetylene black, obviously as a result of the favorable pore structure and considerable surface area of this carrier.

The effect of metal content on structural properties and performance of catalysts was studied with ruthenium-platinum alloys (1:4) supported on activated carbon. As illustrated in Table 20, an increase in crystallite size and bulk density occurs with increasing metal content, in the range from 25% to 75% by weight. With this high surface area carrier the highest activity, however, was obtained with a 50% metal content.

c. Thermal Stability of Carbon Supported Catalysts

The data shown below illustrate the beneficial effect of (carbon) carriers on the stability of electro-catalysts. Thermal aging is recognized as one of the major reasons for the decrease in electrode activity observed during the operation of fuel cells at elevated temperatures (25). The stability of catalysts was determined by heating in hydrogen to temperatures up to 400°C. Crystallite sizes and activities for methanol oxidation were subsequently determined in phosphoric acid or sulfuric acid.

Platinum, platinum-rhodium and platinum-iridium alloys supported on activated carbon: In Table 23 the effect of heating in hydrogen on crystallite size is illustrated for the temperature range from 120°C to 300°C. The stability of the catalysts evaluated appears to be comparable up to a temperature of 120°C. At higher temperatures, however, platinum exhibits a lower stability than the alloyed samples. In either case a marked increase in crystallite size is notable. The activity of thermally aged catalysts for methanol oxidation at 140-150°C in phosphoric acid is shown in Tables 24, 25. A decline in performance may be observed for platinum-rhodium samples particularly at higher current densities. In contrast, platinum supported on carbon exhibited unexpectedly an improved activity after heating in hydrogen despite strong crystallite growth upon heating to 200°C.

Platinum-ruthenium alloy supported on activated carbon: Platinum-ruthenium alloys with a ruthenium content ranging from 5-30% by weight were supported on activated carbon and acetylene black and tested for thermal stability. As a rule, the aging process was studied on catalysts in powder form which were heated in hydrogen to temperatures from 120-400°C for two hours to accelerate recrystallization. Changes in crystallite size, bulk density and activity for methanol oxidation were recorded after the heat treatment.

Pertinent crystallite size, bulk density and activity data for platinum-ruthenium alloys with 20% and 30% ruthenium based on the metal content are summarized in Tables 26, 27. An increase in crystallite size may be observed on both samples after heating to 120°C. A heat treatment of the original sample at 200°C, peculiarly, only causes recrystallization of the sample containing 20% ruthenium based on the precious metal content, whereas the crystallite size is unchanged in the preparation containing 30% ruthenium. Furthermore, after aging at 300°C and 400°C the crystallite size observed is not materially different from that attained at 200°C. These findings are possibly related to an interaction of hydrogen with the ruthenium alloy. Hydrogen is known to have a considerable solubility in ruthenium which may have an effect upon the recrystallization process. Further studies are required to elucidate these observations.

Crystallite size data correlate in general with the performance of catalysts for the oxidation of methanol. The 20% ruthenium sample (Table 26) shows lower activity after heating to 120°C and 200°C, whereas treatment at 300°C and 400°C does not markedly alter performance. The activity is also consistent with crystallite size in the sample containing 30% ruthenium based on the precious metal content (Table 27) except for the unheated preparation which exhibited lower activity than heated catalysts of comparable crystallite size. These findings may be attributed to a lowering in bulk density which takes place upon heating.

Platinum-ruthenium alloy on acetylene black:
Crystallite size, bulk density and activity data for various platinum-ruthenium alloys deposited on acetylene black are summarized in Tables 28, 29. Catalysts contain from 5-30% ruthenium based on the precious metal content. The stability of these preparations is somewhat inferior to alloys supported on activated carbon, which undoubtedly is due to the lower surface area of acetylene black. The activity of the catalysts, however, is considerably higher than observed on activated carbon, considering the lower catalyst loadings employed in testing.

It is interesting to note that catalytic activity decreases to a lesser degree than to be expected from the changes in crystallite size. This may be attributed partly to the decrease in bulk density which takes place upon heating whereby additional surface area may be exposed. Possibly also, the surface lost due to recrystallization is primarily in micropores which contribute little to the over-all activity.

The thermal stability of catalysts improves with increase in ruthenium content. These findings are in agreement with studies on unsupported platinum-ruthenium alloys which indicated less recrystallization upon heating at higher ruthenium concentrations (page 19).

3. Platinum Supported on Miscellaneous Substrates

Some preliminary studies have been made with substrates discussed on page 22. Platinum was supported in a concentration of 50% by weight. The carriers were used as obtained commercially and no effort was made as yet in preparing such materials with an optimized surface development and pore structure. A summary of the pertinent characteristics of the catalysts prepared is given in Table 30. The data illustrate that platinum may be successfully supported on carriers of relatively low surface area. In all samples a considerable reduction in crystallite size was found compared to unsupported platinum black. The catalyst preparations were tested for the reduction of oxygen in 30% sulfuric acid at 80°C. A slight improvement in performance was obtained with boron carbide, silicon carbide, and tantalum oxide supported samples compared to platinum black. Polarization decreased from 20 mV (tantalum oxide, silicon carbide) to 40 mV (boron carbide) at a current density of 100 mA/cm².

V. CONCLUSIONS

The work carried out in the present contract has been concerned with the relationship between structural factors of precious metal catalysts and their activity. These studies involved notably platinum, iridium, rhodium, ruthenium and alloys thereof. The intrinsic activity of a given catalyst is not easily separable from other factors determining its over-all performance such as geometric factors. But in all cases it appears that for a given catalyst the performance correlates with the magnitude of the "accessible surface" and no evidence has been found that the size of the primary crystals has any further influence beyond affecting surface area. The surface development and the structure of chemically prepared catalysts varies considerably with the catalytic material. Two extremes are platinum and iridium. Platinum black is composed of small but relatively nonporous grains, the surface being well exposed. Iridium black has a high surface area present in a microporous structure of relatively large catalyst grains which thus is not readily available for the electrochemical reaction. Alloy catalysts such as alloys of platinum with iridium, rhodium or ruthenium exhibit a structure which at high platinum content is similar to platinum black. At higher concentrations of the second component however larger catalyst grains are formed and a major fraction of the surface is available in a microporous structure.

For practical purposes alloy catalysts of the platinum ruthenium system or variations thereof appear to be preferable for the fuel electrode. These catalysts exhibit a markedly higher activity than platinum black for the anodic oxidation of various carbonaceous fuels which may be attributed to a high surface area development and a relatively favorable open pore structure. We have, for instance, with a Platinum-Ruthenium anode catalyst and catalyst loadings of 20 mg/cm² been able to operate a fuel cell with humidified propane and oxygen at a stable output (included all IR losses) of .5 volts at 100 mA/cm² corresponding to between 45 to 50% efficiency at a power density of 50m watt/cm². When platinum black was used at the anode under otherwise the same conditions, the cell voltage was only .4 volts. Platinum, however, was the preferred catalyst for the cathode exceeding iridium, rhodium as well as alloyed catalysts markedly in performance. Obviously, considering platinum for the air electrode and platinum-ruthenium for the fuel anode the development of practical fuel cell systems appears feasible on the basis of above mentioned results if the catalytic precious metal component could be sufficiently diluted and stabilized.

Preparations using various types of carbon as model substrates have shown improved activity as a result of an increase in metal surface area and a better accessibility of the active metal surface. This applies particularly to alloy catalysts which in the unsupported state may have a microporous structure and consequently poorly accessible surface. A carbon substrate of low porosity and small particle size yielded superior activity due to improved mass transport.

The carriers were also shown to increase the stability against thermal aging and, thereby, to increase the life of precious metal catalysts.

Any practical use of carbon substrates is limited, however, to the fuel electrode where stability up to potential of at least .5V vs. hydrogen has been demonstrated. Under cathodic conditions carbon is oxidized when it is in contact with platinum metals. Alternative carriers with sufficient chemical stability in hot phosphoric acid are tungsten, tantalum or alloys thereof as well as selected intermetallic compounds all of which have a conductivity 10-100 times that of carbon. Certain base metal oxides such as tantalum oxide or tungsten oxide also appear to qualify as carriers. No dissolution or recrystallization was observed in hot phosphoric acid.

VI. RECOMMENDATIONS

Continued research is recommended towards the development of diluted precious metal catalysts on suitable supports leading to active catalysts noble under conditions of use. Specifically, platinum should be considered for the oxygen electrode and the platinum-ruthenium system or variations thereof for the fuel anode.

Carrier Materials: Carbon may serve as a model material since it is available in a variety of types differing in shapes, particle size, surface areas and pore structures. In addition, carbon may be useful particularly for the fuel electrode due to stability at potentials up to .5 volts vs. hydrogen. Further considered as supporting materials may be oxides particularly those of tantalum or tungsten which are stable in hot phosphoric acid. Utility of oxides as carriers is contingent however on finding ways of producing these carriers with suitable surface and low porosity and depositing the catalytic metals in form of continuous films to insure sufficient electrical conductivity.

A superior metal dispersion than possible on non-conductive oxides might be obtained possibly on substrates consisting of metals, alloys or certain intermetallic compounds.

Tantalum, tungsten, various carbides and silicides were shown to have adequate acid stability and a conductivity exceeding that of carbon 10-100 times.

Since practically all these materials form non-conductive oxide films, techniques have to be developed to deposit the catalytic metal in direct contact with the bulk material. The resulting catalysts are expected to contain lower concentrations of precious metals than would be possible with non-conducting carriers.

VII. IDENTIFICATION OF KEY
TECHNICAL PERSONNEL

The following technical personnel have been working on the fuel cell contract for the quarterly period of September, October, and November 1964:

O. J. Adlhart, Ph.D., Head of Fuel Cell
Development Section - 467 hours

M. J. Halpern, Ph.D. in Physical Chemistry
- 40 hours

M. M. Hartwig, Ph.D. in Chemistry - 312 hours

H. K. Straschil, Ph.D., Head of Gas Processing
Section - 73 hours

A. J. Haley, Head of Surface Chemistry Section
- 32 hours

D. J. Accinno, Head of Metallography Section
- 17 hours

Technicians - 1202 hours

VIII BIBLIOGRAPHY

- (1) Engelhard Industries, Inc., Contract No. DA-36-039 SC-90691 Final Report No. 4.
- (2) Haley, A. J., Continuous Flow Method of Surface Area Measurement, J. of Applied Chemistry, 13 392-399 (1963).
- (3) Will, F. G. and C. A. Knorr, Z. Elektrochemie 64 258 (1960).
- (4) Robell, A. J., E. V. Ballou, M. J. Boudart, Surface Diffusion of Hydrogen on Carbon. Preprints of Papers of the Journal of Physical Chemistry, 38th National Colloid Symposium, June 1964.
- (5) California Research Corp., Investigation Study Relating to Fuel Cells, ARPA Contract No. DA-49-186-ORD-929, Report 10, p. 93.
- (6) General Electric Co., USAEDL, Saturated Hydrocarbon Fuel Cell Program, Interim Report No. 9.
- (7) Juliard, A. L. and H. Shalit, J. Electrochem. Soc. 110 1002 (1963).
- (8) Tyco Laboratories, Inc., Electrochemistry of Fuel Cell Electrodes, Technical Memorandum No. 8, Report to Office of Naval Research, Contract No. NONR-3765(00).
- (9) American Oil Co., Basic Study of Sorption of Organic Fuels During Oxidation at Electrodes, Contract No. DA-11-022-ORD-4023, Reports 1-9.
- (10) Reinmuth, W., Electrochemical Relaxation Techniques, Analytical Chemistry Annual Review, Reference 211R (1964).
- (11) Engelhard Industries, Inc., Contract No. DA-36-039 SC-90691, Report No. 4, p 30.
- (12) Giner, J., J. Electrochem. Soc. 111 376 (1964).
- (13) Engelhard Industries, Inc., Contract No. DA-36-039 SC-85043 Final Report No. 4, pp 15-18.
- (14) Engelhard Industries, Inc., Contract No. DA-36-039 SC-85043 Final Report No. 4, p 7.
- (15) Dahms, H. and J. O'M. Bockris, The Relative Electrocatalytic Activity of Noble Metals in the Oxidation of Ethylene, J. of the Electrochem. Soc., 111 p 728 (1964).
- (16) Engelhard Industries, Inc., Contract No. DA-36-039 SC85043 Final Report No. 4, Table 18.

- (17) Schwab, G. M. and R. H. Griffith, Alterung von Katalysatoren, Handbuch der Katalyse, Vol. IV, pp. 326-330, Springer (1943).
- (18) McKee, D. W., J. Phys. Chem., 67 1336 (1963).
- (19) American Cyanamid Co., Research and Development of High Performance Light Weight Fuel Cell Electrodes, NASA 3-2786 p. 21, January 1964.
- (20) Engelhard Industries, Inc., Contract No. DA-36-039 AMC-03700(E), Report No. 1, pp. 10-12.
- (21) Schwarzkopf and Kieffer, Refractory Hard Metals, 1953, McMillan Co.
- (22) Union Carbide Corp., Contract No. DA-36-039 AMC-02314(E), Thin Fuel Cell Electrodes, Report 1.
- (23) General Electric Co., Materials of Construction for Hydrocarbon Fuel Cells, ARPA Contract DA-44-009 AMC-479(T). Report No. 1.
- (24) California Research Corp., Investigate Study Relating to Fuel Cells, Contract No. DA-49-186 ORD-929.
- (25) General Electric Co., Hydrocarbon - Air Fuel Cells. Contracts: Nos. DA 44-009 ENG-4909, DA 44-009 ENG-477(T).

Appendix A

TABLES

TABLE 1

Surface Area of Platinum Metal Catalysts
Determined by Potential Sweep Coulometry

Catalyst* Composition in Weight %	Coulometric Surface m ² /g		BET m ² /g	Calculated from Crystallite Size
	Anodic	Cathodic		
Pt	24	24.3	24	30
Pt 95 Ir 5	33	32	38	55
Pt 95 Rh 5	39	33	43	63
Rh	-	62	80	91

* Chemically reduced metal blacks

TABLE 2

Surface Area* of Platinum
Supported on Acetylene Black

Catalyst Composition Weight %	Heat ** Treatment of Catalyst	Cathodic Coulometry m ²	Chemisorption	Calculated from Crystal- lite Size m ²	BET m ²
Pt 50 C 50	not heated	50	46	44	92
Pt 50 C 50	120°C	40	29.4	36	-
Pt 50 C 50	200°C	36	20.8	18	74

* All surface area data are given for 2 g of catalyst corresponding to 1 g of platinum.

** Catalyst were heated two hours in hydrogen.

TABLE 3
Spectroanalysis of a Pt 80 Ru 20 Alloy Catalyst

Impurities in Wt.%

* Pd	.3-.4	Au	N.D.
* Ir	.01-.02	Ag	.0003
* Rh	.002	Pb	.004
* Cu	.01-.02	Sn	.003
* Si	.006	Zn	N.D.
* Al	.03	Fe	.008
* Ni	.01-.02	Mn	.001
* Cr	.01	Mg	.002
* B	.02	Ca	.001

* Values uncertain due to interference by Ru, Pt or Pd lines.

N.D. = Not Detected

TABLE 4

Physical Characteristics of
Platinum, Iridium and Rhodium Black

Catalyst	Coulometric Surface m^2/g	BET m^2/g	Calculated from Crystallite Size m^2/g	Bulk Density g/cm	Crystallite Size \AA
Platinum	24	25	30	.55	100
Iridium	58	99	166	2.07	16
Rhodium	66	80	86	.61	53

TABLE 5
Physical Characteristics of
Unsupported Platinum Alloy Catalysts

Catalyst Composition in Weight %	Surface Area (m ² /g)			Crystallite Size (Å)	Bulk Density (g/cm ³)
	a)	b)	c)		
Platinum	24	25	30	100	.55
Pt 95 Ir 5	33	38	55	56	.74
Pt 95 Rh 5	39	43	63	47	.83
Pt 95 Ru 5	40	48	66	45	1.09

a) measured electrochemically

b) measured by gas adsorption

c) calculated from crystallite size

TABLE 6

Methanol Oxidation on Platinum Metal Blacks

Temperature: 140-180°C
Electrolyte: 85% phosphoric acid
Catalyst Loading: 50 mg/cm²

Catalyst	Potential in Volts vs. HE Current Density mA/cm ²				
	0	10	20	50	100
Platinum	.08	-	.30	.36	.41
Iridium	.07	.15	.21	.33	.39
Rhodium	.10	.38	.39	.46	.50

TABLE 7

Propane Oxidation on Platinum Metal Blacks

Temperature: 150°C
Electrolyte: 85% phosphoric acid
Catalyst Loading: 50 mg/cm²

Catalyst	Potential in Volts vs. HE Current Density mA/cm ²				
	0	10	20	50	100
Platinum	.11	.19	.24	.34	.43
Iridium	.09	.38	-	-	-
Rhodium	.10	.32	.44	-	-

TABLE 8


Oxidation Potentials for Methanol
on Unsupported Platinum Alloy Catalysts

Temperature: 140-150°C
Electrolyte: 85% phosphoric acid
Fuel: 4% methanol in nitrogen
Catalyst Loadings: 50 mg/cm²

Catalyst Composition	Potential in Volts vs. HE Current Density mA/cm ²				
	0	20	50	100	130
Pt 95 Ru 5	.07	.13	.20	.27	.30
Pt 95 Ir 5	.08	.23	.28	.34	.36
Pt 95 Rh 5	.06	.27	.34	.41	.47
Pt	.08	.30	.36	.41	.44

TABLE 9

Performance Data for Various
Fuels on Platinum Black Catalysts

Test Temperature	- 165°C
Pressure	- Atmospheric
Catalyst Loadings	- 20 mg/cm ²
Electrolyte Resistance/cm ²	- 27x10 ⁻² 
Anode	- Pt black
Cathode	- Pt black
Electrode Size	- 20 cm ²
Oxidant	- Tech. Grade Oxygen

Fuel	Water Vapor Sat. Temp. °C	Cell Voltage in Volts *(incl. I.R. drop) Current Density mA/cm ²						
		0	20	30	50	75	100	150
Hydrogen	dry	1.03	.96	.94	.91	.88	.86	.80
Ethane	83	.90	.62	.59	.53	n.t.	n.t.	n.t.
Propane	83	.92	.67	.61	.54	.46	.39	n.t.
Butane	85	.90	.64	.59	.53	n.t.	n.t.	n.t.
Carbon Monoxide	83	1.01	.64	.42	n.t.	n.t.	n.t.	n.t.

* Reproducibility ± 15 mV at current densities > 50 mA/cm²
with hydrocarbons less at lower current.

n.t. = not tested

TABLE 10

Performance Data for Various
Fuels on Pt 95 Ru 5 Catalysts

Temperature - 165°C
 Pressure - Atmospheric
 Catalyst Loadings - 20 mg/cm²
 Electrolyte Resistance/cm² - 27x10⁻²
 Oxidant - Tech. Grade Oxygen
 Anode - Pt 95 Ru 5
 Cathode - Pt
 Total Electrode Area - 20 cm²

Fuel	Water Vapor Sat. Temp. °C	Cell Voltage in Volts incl. I.R. Drop Current Density mA/cm ²						
		0	20	30	50	75	100	150
Hydrogen	dry	1.03	.96	.94	.91	.88	.86	.80
Ethane	83	.92	.73	.69	.63	.55	n.t.	n.t.
Propane	83	+.90	.73	.69	.62	.55	.50	n.t.
Butane	85	+.90	n.t.	.65*	.61	.55	n.t.	n.t.
Carbon Monoxide	83	1.02	.63	.57	.48	n.t.	n.t.	n.t.
Ethylene	83	n.t.	.52	n.t.	.44	n.t.	n.t.	n.t.

n.t. = not tested

* - 40 mA/cm²

TABLE 11

Typical Composition of Anode
Effluent from Propane Oxidation

Temperature - 165°C
 Electrode Area - 20 cm²
 Flow Rate - 9 cm³ +10%
 Catalyst Loading - 20 mg/cm²
 Catalyst Composition - Pt or Pt 95 Ru 5

Anode Catalyst		Pt	Pt-Ru	Pt	Pt-Ru	Pt-Ru	Pt-Ru
All current in mA		0	0	1000	1000	1000	2100
Composition of feed Vol %**	C ₃ H ₈	99+	99.9+	99+	99.9+	99+	99+
	CH ₄	.02	n.d.*	.02	n.d.	.02	.02
	C ₂ H ₆	.7	n.d.	.7	n.d.	.7	.7
Composition of effluent Vol %**	C ₃ H ₈	97.9	99.8	81.9	87.2	83.9	70.8
	CH ₄	.02	n.d.	.02	n.d.	.02	.02
	C ₂ H ₆	.6	n.d.	.5	n.d.	.6	.6
	CO ₂	1.5	.2	17.6	12.8	15.5	28.6

* n.d. - not detected

** Dry basis

TABLE 12

Typical Composition of Anode Effluent
from Ethylene and Ethane Oxidation

Temperature - 165°C
 Electrode Area - 20 cm²
 Flow Rate - 9 cm³ $\pm 10\%$
 Catalyst Loading - 20 mg/cm²
 Catalyst Composition - Pt or Pt 95 Ru 5

Anode Catalyst		Pt	Pt	Pt-Ru	Pt-Ru
All current in mA		0	1000	1000	500
Composition of feed Vol %**	C ₂ H ₆	99+	99+	99+	.1
	C ₂ H ₄	.5	.5	.5	99+
	C ₃ H ₈	.2	.2	.2	n.d.
	CH ₄	n.d.*	n.d.	n.d.	.08
	CO	n.d.	n.d.	n.d.	n.d.
Composition of effluent Vol %**	C ₂ H ₆	98.	87.9	84.9	.1
	C ₂ H ₄	.2	n.d.	n.d.	95.3
	C ₃ H ₈	.2	.2	.2	n.d.
	CH ₄	n.d.	n.d.	n.d.	.08
	CO	-	-	-	.04
	CO ₂	1.6	11.9	14.9	4.5

* n.d. - not detected

** Dry basis

TABLE 13

Comparative Performance of Unsupported
Platinum Metal Catalysts for Oxygen Reduction

Temperature - 80°C
 Electrolyte - 7.5 N sulfuric acid
 Catalyst Loadings - 10 mg/cm²
 Atmospheric pressure oxygen

Catalyst Composition	BET Surface Area m ² /g	Potential in Volts vs. HE Current Density mA/cm ²					
		0	10	20	30	50	100
Pt	16-27	1.02	.96	.90	.87	.85	.78-.83
Ir	99	.92	.83	.77	.74	.70	.58
Rh	80	.91	.80	.74	.71	.65	.54
Pt 99 Ru 1	37.5	1.02	.96	.91	.89	.85	.80
Pt 95 Ru 5	48.1	.98	.91	.86	.83	.78	.70
Pt 95 Ir 5	38	.97	.91	.85	.83	.77	.67
Pt 95 Rh 5	43	.97	.91	.86	.82	.76	.66

TABLE 14

Thermal Aging of Unsupported
Platinum Metal Catalysts

Catalyst Composition Weight %	Thermal Treat- ment*	Pt	Rh	Pt 95 Ir 5	Pt 95 Rh 5
Surface Area (BET) m ² /g	none	14	80	38	43
	120°C	8	55	19	17
Crystallite Size in Å	none	101	53	56	47
	120°C	132	62	78	84
Bulk Density g/cm ³	none	.55	.61	.74	.83
	120°C	.70	.64	1.51	1.57

* Catalysts were heated to 120°C for 2 hours in hydrogen atmosphere.

TABLE 15

Thermal Aging of Unsupported
Platinum-Ruthenium Catalysts

Catalyst Composition Weight %	Surface Area in m^2/g (BET)	
	No Heat Treatment	Heated to 120°C for 2 hrs. in Hydrogen Atmosphere
Pt 100	14	8
Pt 99 Ru 1	37.5	15.9
Pt 95 Ru 5	48.1	19.7
Pt 90 Ru 10	67	22
Pt 60 Ru 40	68	12

TABLE 16

Characteristics of Various Prospective Carrier Materials

Carrier	Specific R of massive specimen (Literature) Microhm/cm	Measured R on compacted powders Microhm/cm	Particle size in microns	Surface area in m ² /g	Bulk density in g/cm ³
Molybdenum disilicide	18.9	776.10 ³	3-8	.5	3.5
Chromium disilicide	-	-	4-8	.5	2.59
Titanium disilicide	12.3	-	3-10	.64	2.25
Zirconium disilicide	16.1	-	<35	.52	2.79
Tantalum disilicide	8.5	135.10 ³	<35	.57	4.06
Chromium boride	8.5	-	3-10	.31	3.22
Tantalum oxide	-	-	<35	3.0	1.22
Tungsten oxide	-	-	<35	16.0	2.95
Silicon carbide	-	-	<35	1.4	1.17
Boron carbide	300-800	1150.10 ³	3	13.2	.45
Chromium carbide	-	-	<35	-	-
Tantalum carbide	30	-	<35	-	-
Tungsten carbide	80	700.10 ³	<35	.55	3.76
Tantalum	12.4	350.10 ³	<35	4.3	-
Tungsten	5.6	31.10 ³	<35	3.5	-

TABLE 17

Stability of Platinum Activated Carbon and
Selected Carbides Under Oxidizing Conditions

Test Arrangement: Full cell (Fig. 9)
 Anode Feed : Humidified nitrogen (400 mm HgH₂O)
 Cathode Feed : Dry Oxygen
 Electrode Area : 20 cm²
 Flow Rate : Approx. 15 cm³/min.

Catalyst Composition Weight %	Temperature °C	Carbon Dioxide Content in Cathode Effluent in ppm	
		Open Circuit	50 mA/cm ²
Pt 50 C* 50	100	290	-
	150	4400	380
Pt 50 B ₄ C 50	100	600	-
	150	820	-
Pt 50 SiC 50 Pt 50 WC 50	150	580	-
	150	700	-

* Acetylene Black

TABLE 18

Crystallite Size and Bulk Density of Platinum, Iridium
and Rhodium Containing Catalysts Supported on Carbon

Catalyst Composition in Weight %	Type of Carbon Support	Bulk Density g/cm ³	Crystallite Size Å
Pt 50 C 50	Activated Carbon	.64 (.55)	59 (100)
Pt 50 C 50	Acetylene Black	.16 (.55)	59 (100)
Ir 50 C 50	Activated Carbon	.67 (2.07)	17 (17)
Pt 35 Ir 15 C 50	" "	.64	37 (56)*
Pt 35 Rh 15 C 50	" "	.69	32 (47)**
Pt 40 Rh 10 C 50	" "	.62	32

Figures in parenthesis show crystallite size and bulk density of unsupported blacks.

* Catalyst composition 95% Pt 5% Ir

** Catalyst composition 95% Pt 5% Rh.

TABLE 19

Crystallite Size and Bulk Density of
Platinum-Ruthenium Catalysts Supported on Activated Carbon

Composition Weight %	Crystallite Size Å	Bulk Density g/cm ³
Pt 50 C 50	59 (100)	.64 (.55)
Pt 47.5 Ru 2.5 C 50	32 (45)	.76 (1.09)
Pt 40 Ru 10 C 50	15 (35)	.76 (1.5)
Pt 35 Ru 15 C 50	18 (30)	.73 (2.5)

Figures in parenthesis show crystallite size and bulk density of unsupported blacks.

TABLE 20

Effect of Carbon Support on Physical
Properties of Platinum-Ruthenium Catalysts

Carbon Support	Surface Area of Support m ² /g	Metal Content of Catalyst Weight %	Crystallite* Size of Catalyst Å	Bulk Density of Catalyst g/cm ³
LTV 230	15.5	50	34	1.03
LTV 239	8.5	50	32	1.25
Acetylene Black	75-80	50	16	.32
Activated Carbon	958	50	19	.75
"	958	25	amorphous	.58
"	958	75	25	1.21

* Crystallite size of unsupported catalyst is 30 Å.

TABLE 21

Methanol Oxidation on Platinum Metal
Catalysts Supported on Activated Carbon

Test Conditions - Pt-metal Loadings: 9 mg/cm²
 Temperature: 140-150°C
 Electrolyte: 85% phosphoric acid
 Fuel: 4% methanol in nitrogen

Catalyst Composition Weight %	Anode Potential in Volts vs. H ₂ in Same Electrolyte Current Density mA/cm ²				
	0	10	20	50	100
Pt 50 C 50	.11	-	.27	.34	.41
Ir 50 C 50	.15	.31	.33	.36	.44
Pt 40 Rh 10 C 50	.10	-	.24	.31	.42
Pt 35 Rh 15 C 50	.16	-	.23	.26	.30
Pt 40 Ru 10 C 50	.07	.13	.17	.25	-
Pt 35 Ru 15 C 50	.07	-	.13	.17	.21
Pt 35 Ir 15 C 50	.13	-	.34	.40	.44

TABLE 22

Effect of Carbon Support on
Performance of Pt and Pt-Ru Catalysts

Test Conditions: Fuel - Methanol (2 Vol %)
 Electrolyte - 2 N H₂SO₄
 Temperature - 90°C
 Catalyst Loadings - 20 mg/cm²
 precious metal
 Pt 35 Ru 15 C 50

Carbon Support **	Potential in Volts vs. hydrogen in same electrolyte Current Density mA/cm ²						
	0	12	20	30	50	100	200
Activated Carbon	.08	.18	.22	.26	.27	.34	.42
LTV* 230	.11	.14	.23	.27	.35	.41	.48
LTV* 239	.05	.13	.18	.20	.24	.33	.42
Acetylene Black	.07	.19	.21	.24	.27	.33	.37

* Ling Temco Vought

** Metal content 50% by weight

TABLE 23

Thermal Stability of Carbon
Supported Platinum Alloy Catalysts*

Catalyst Composition Weight %	Not Heated	Crystallite Size Å		
		120°C	200°C	300°C
Pt 50 C 50	59	84	192	-
Pt 40 Rh 10 C 50	32	44	70	141
Pt 35 Rh 15 C 50	32	45	71	124
Pt 35 Ir 15 C 50	37	43	-	-

* Catalysts were heated 2 hours in hydrogen atmosphere.

TABLE 24

Effect of Heating on Activity of Platinum
Supported on Activated Carbon for Methanol Oxidation*

Electrolyte: 85% phosphoric acid
 Temperature: 140-150°C
 Fuel: 4% methanol in nitrogen
 Platinum Loadings: 9 mg/cm²

Heat Treatment	Potential in Volts vs. H ₂ Current Density mA/cm ²				
	0	10	20	50	100
none	.11	-	.27	.34	.41
120°C	.09	-	.26	.32	.49
200°C	.11	.21	.25	.31	.38

* Catalysts were heated for 2 hours in hydrogen

TABLE 25

Effect of Heating on Activity of
Pt 35 Rh 15 C 50 on Activated Carbon for Methanol Oxidation*

Electrolyte: 85% phosphoric acid
 Temperature: 140-150°C
 Fuel: 4% methanol in nitrogen
 Pt metal loadings: 9 mg/cm²

Heat Treatment	Potential in Volts vs. HE Current Density mA/cm ²				
	0	10	20	50	100
none	.10	-	.23	.26	.300
120°C	.09	.17	.20	.26	.320
200°C	.09	.19	.26	.34	.420
300°C	.10	.23	.26	.34	.430

* Catalysts were heated for 2 hours in hydrogen.

Effect of Heating on Physical Characteristics and Performance of Pt 40 Ru 10 C* 50 Catalysts

Temperature** °C	Crystallite Size in Å	Bulk Density g/cm ³	Potential in Volts vs. HE Current Density mA/cm ²				
			0	20	30	50	100
not heated	15	.76	.09	.20	.22	.25	.31
120	27	.74	.10	.20	.22	.26	.33
200	41	.73	.09	.23	.26	.30	.38
300	39	.73	.09	.24	.26	.30	.37
400	42	.73	.10	.25	.28	.32	.39

** Catalysts were heated for two hours in hydrogen.

TABLE 27

Effect of Heating on Physical Characteristics
and Performance of Pt 35 Ru 15 C* 50 Catalysts

Test Conditions: 2 N H₂SO₄ + 2 Vol % Methanol
Temperature - 90°C
Catalyst Loadings - 20 mg/cm²
precious metal

Temperature** °C	Crystallite Size in Å	Bulk Density g/cm ³	Potential in Volts vs. HE Current Density mA/cm ²				
			0	20	30	50	100
not heated	19	.75	.08	.22	.26	.27	.34
120	44	.69	.09	.22	.24	.27	.34
200	19	.68	.10	.21	.23	.26	.33
300	22	.63	.09	.22	.24	.26	.32

* Activated Carbon

** Catalysts were heated for two hours in hydrogen.

TABLE 28

Effect of Heating on Physical Properties and Performance
of Platinum-Ruthenium Catalysts Supported on Platinum Black

Test Conditions: 2 N sulfuric acid + 2 vol % methanol
Temperature - 90°C
Catalyst Loadings - 12 mg/cm²
precious metal

Catalyst Composition Weight %	Temp.* Heated °C	Crystallite Size Å	Bulk Density g/cm ³	Potential in Volts vs. HE Current Density mA/cm ²				
				0	20	30	50	100
Pt 47.5 Ru 2.5 C 50	not heated	45	.23	.09	.26	.28	.32	.38
Pt 47.5 Ru 2.5 C 50	120	62	.23	.10	.27	.29	.32	.38
Pt 45 Ru 5 C 50	not heated	36	.25	.09	.23	.26	.28	.35
"	120	56	.24	.09	.25	.28	.30	.36
"	200	77	.22	.09	.28	.29	.32	.38
"	300	96	.23	.09	.30	.31	.35	.39

* Catalysts were heated for two hours in hydrogen.

TABLE 29

Effect of Heating on Physical Characteristics
and Performance of Pt 35 Ru 15 Acetylene Black 50 Catalysts

Test Conditions: 2 N H₂SO₄ + 2 Vol % Methanol
 Temperature - 90°C
 Catalyst Loadings - 12 mg/cm²
 precious metal

Temperature* °C	Crystallite Size in Å	Bulk Density g/cm ³	Potential in Volts vs. HE Current Density mA/cm ²				
			0	20	30	50	100
not heated	16	.32	.07	.21	.22	.27	.31
120	30	.33	.07	.21	.23	.27	.32
200	35	.29	.07	.23	.25	.29	.34
300	33	.26	.07	.22	.25	.27	.32

* Catalysts were heated for two hours in hydrogen.

TABLE 30

Characteristics of Platinum Catalysts* Supported
on Miscellaneous Substrates

Catalyst Support	Surface of Substrate m^2/g	Pt Crystallite Size in \AA	Bulk Density of Catalyst g/cm^3
Unsupported Pt	-	100	.55
B ₄ C	13.2	44	.90
SiC	1.4	57	.85
Ta ₂ O ₅	3.0	66	.87
SiO ₂	-	68	.51
W	-	-	2.87

* Platinum content 50% by weight

Appendix B

FIGURES

FIG.1
POTENTIAL SCAN COULOMETER

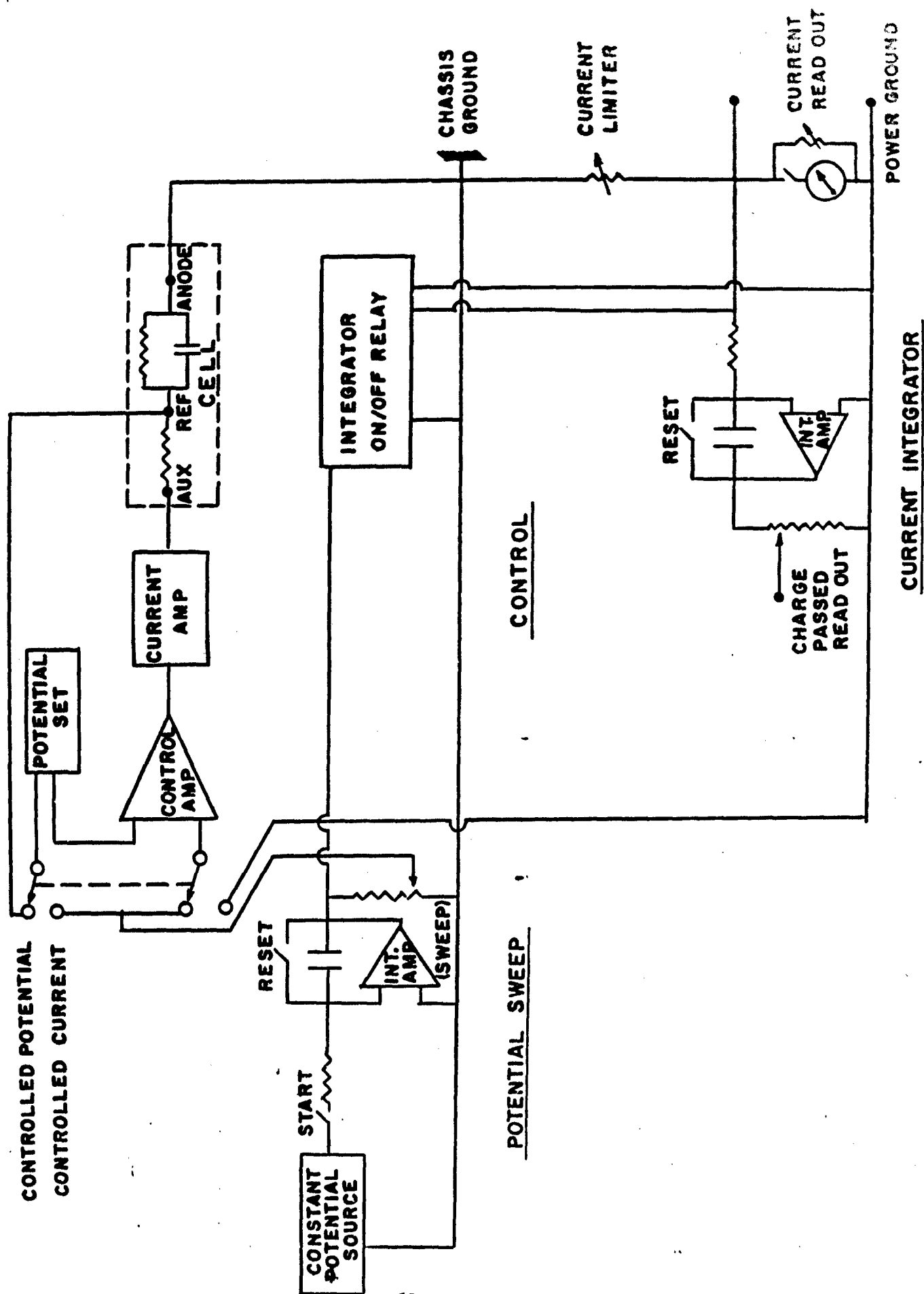


FIG. 2
CURRENT-CHARGE, CURRENT-VOLTAGE CURVES FOR UNSUPPORTED CATALYSTS

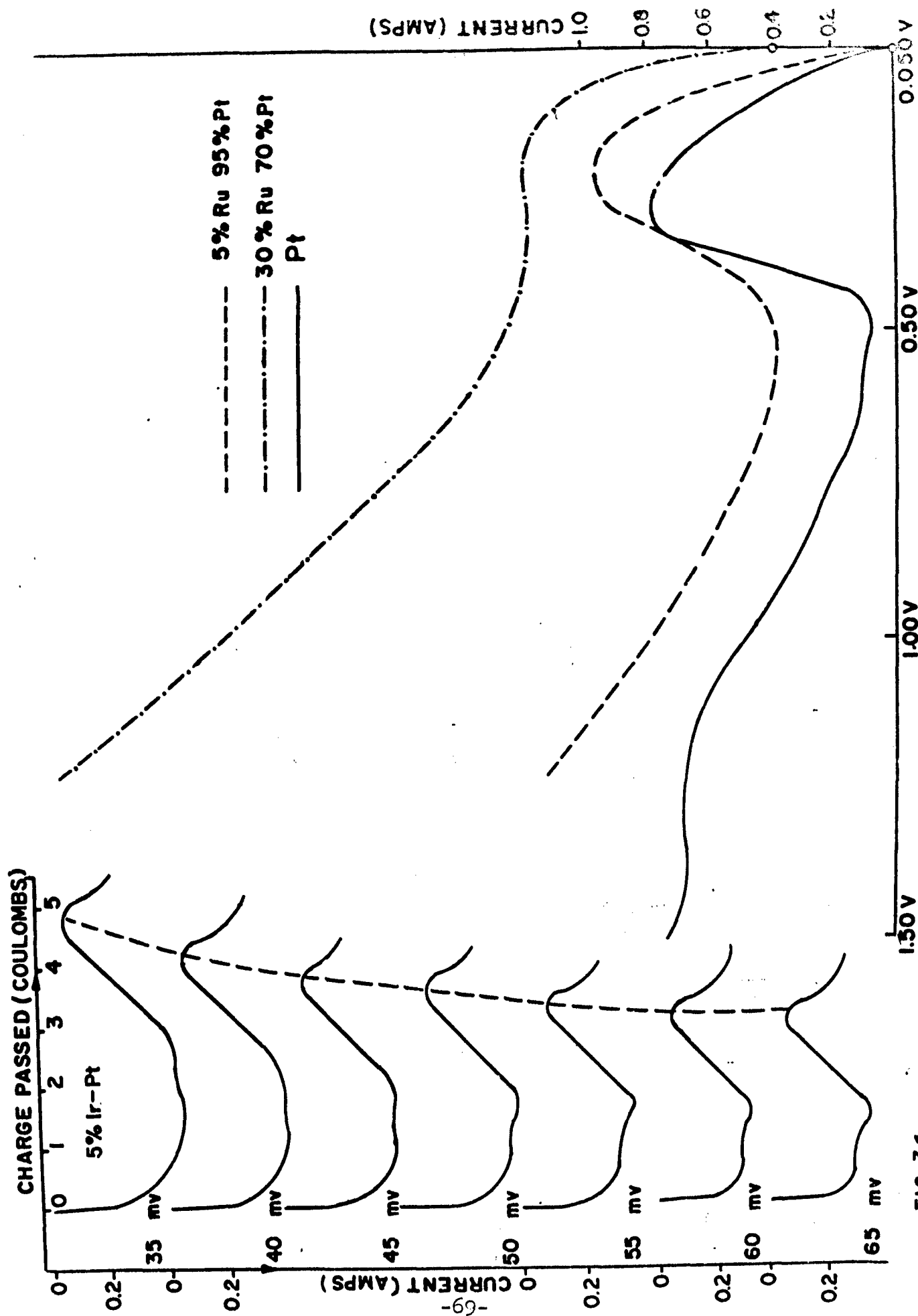


FIG. 3a

FIG. 3b POTENTIAL vs. HYDROGEN

FIG. 3

EFFECT OF SWEEP RATES ON SHAPE OF
CATHODIC-CURRENT CHARGE CURVES

A-BEGINNING OF HYDROGEN EVOLUTION
B-STARTING POINT OF POTENTIAL SWEEP.
(+ 500 mV vs HYDROGEN REFERENCE)

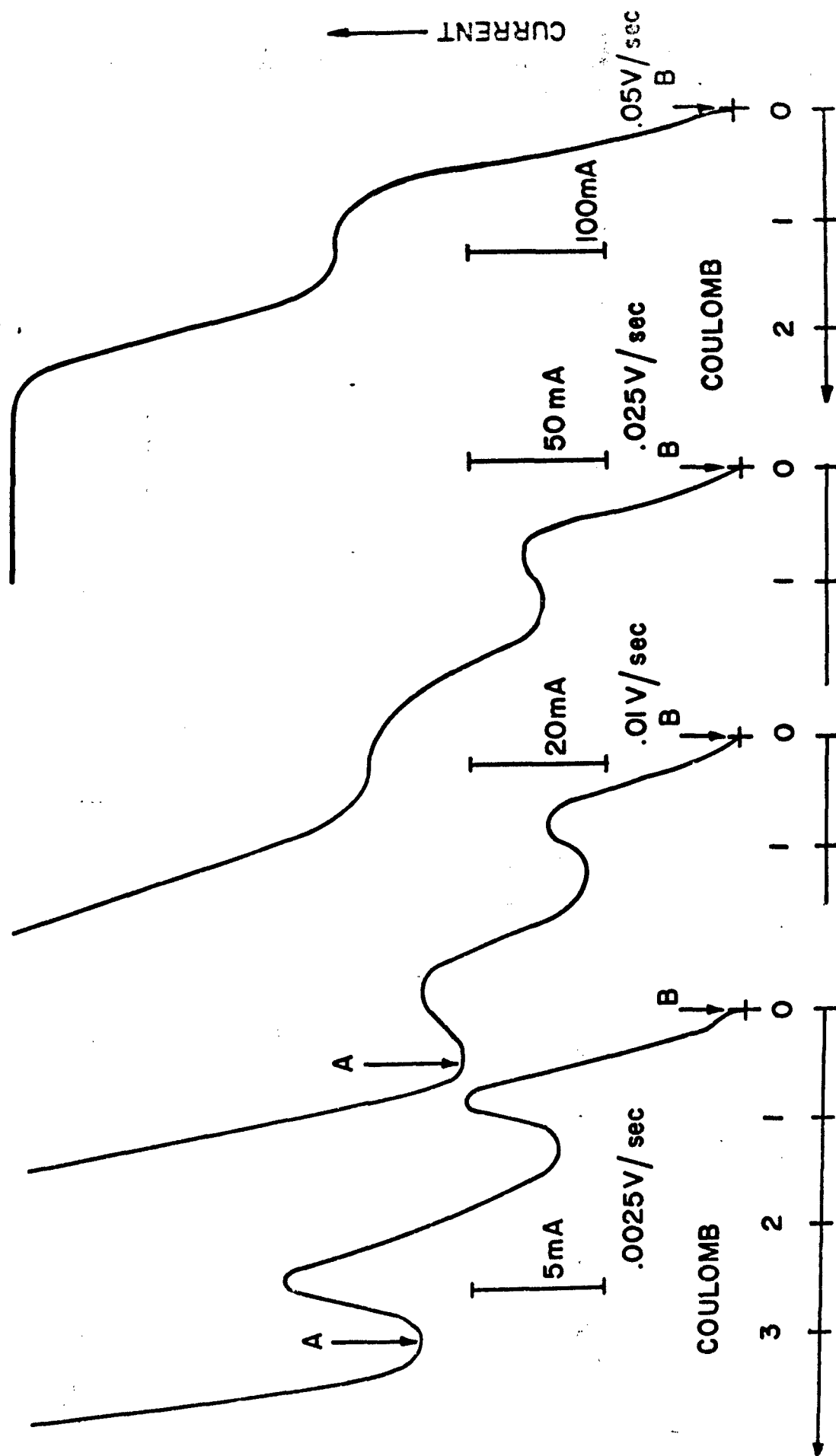
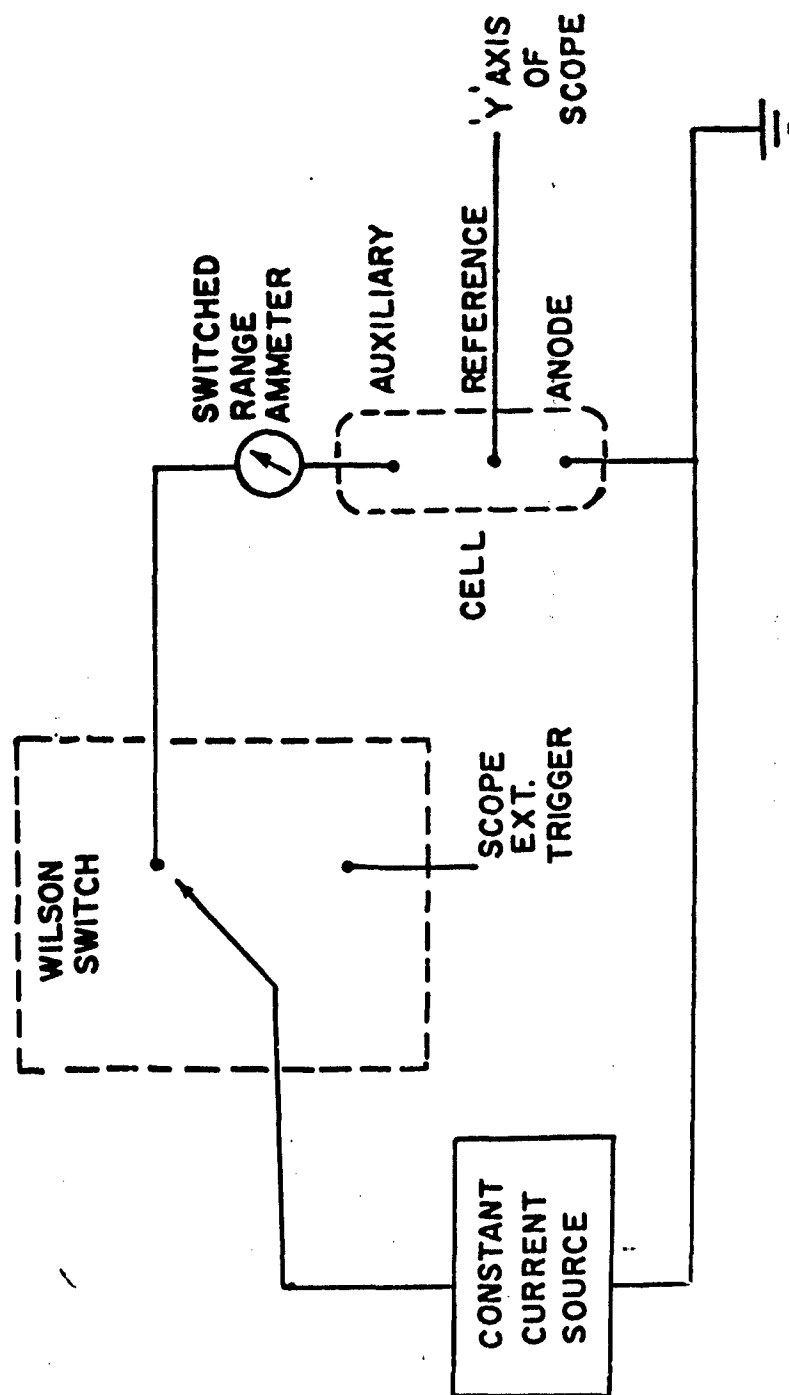


FIG. 4
SQUARE WAVE PULSING

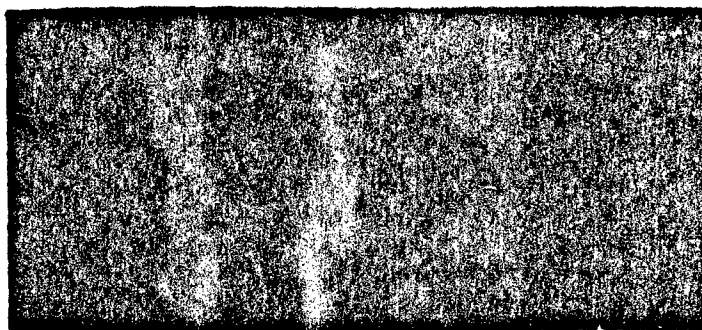


ENGELHARD
INDUSTRIES, INC.

Fig. 5a

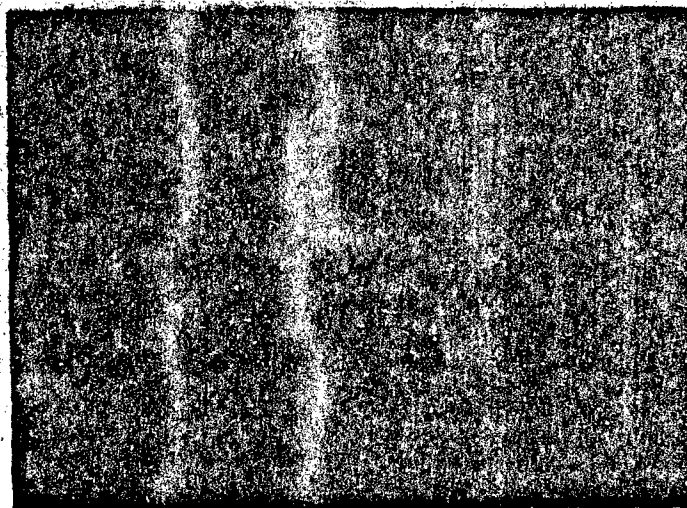
Decay of Polarization for Platinum
Black in Anodic Oxidation of Methanol

100 mv/div



t 10msec/div

100 mv/div



t 50 msec/div

Fig. 5b

FIG. 6

POLARIZATION DECAY CURVE

ANODE: Pt BLACK + TEFLON POWDER (1:1 BY WEIGHT)

ELECTROLYTE: 2N H_2SO_4 , 0.5M METHANOL

TEMPERATURE: 90°C

PULSE: 100 ma/cm² FOR 30 msec

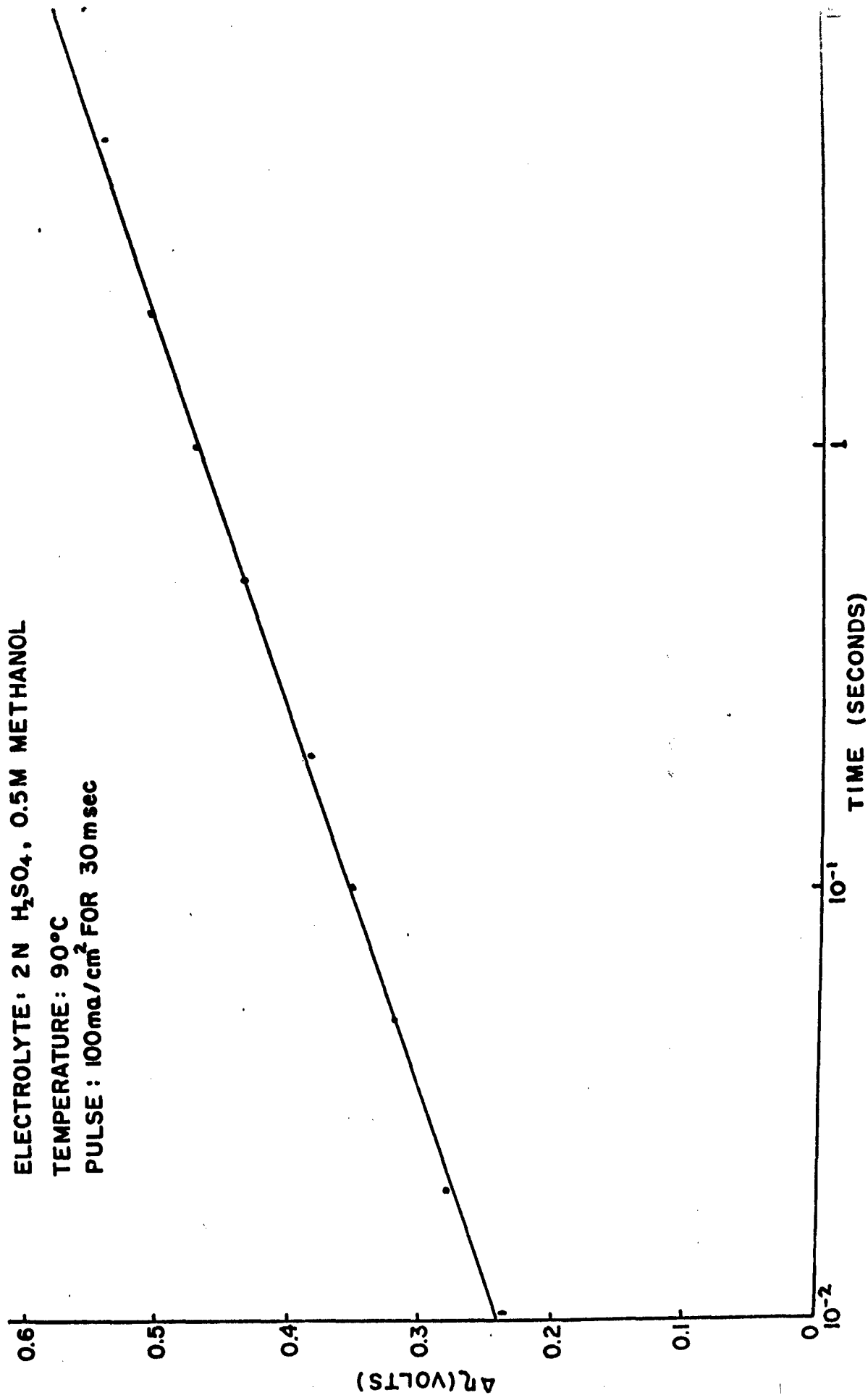


FIG.7
HALF CELL ARRANGEMENT FOR CATALYST EVALUATION

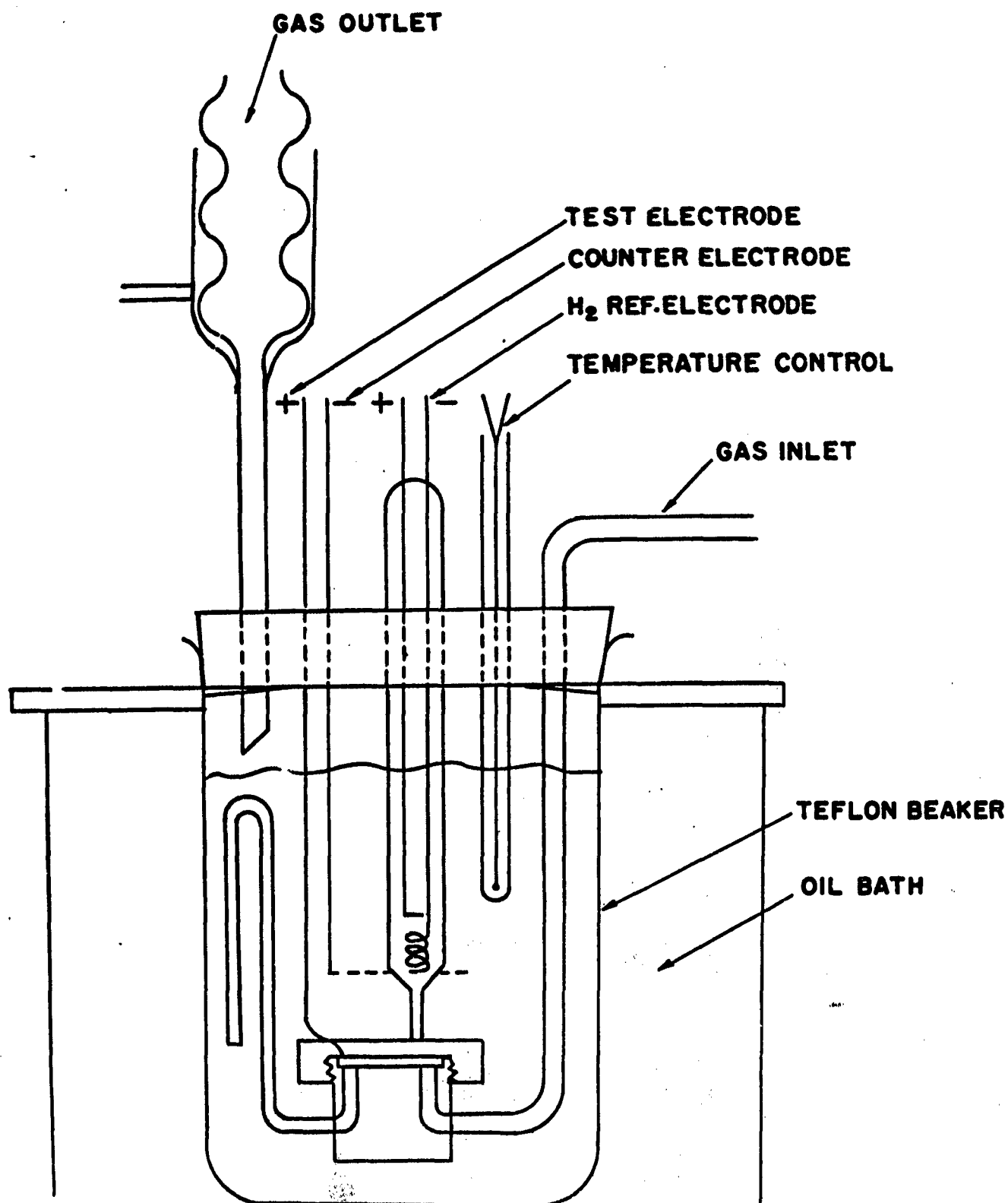


FIG. 8
ARRANGEMENT FOR FUEL CELL TESTING

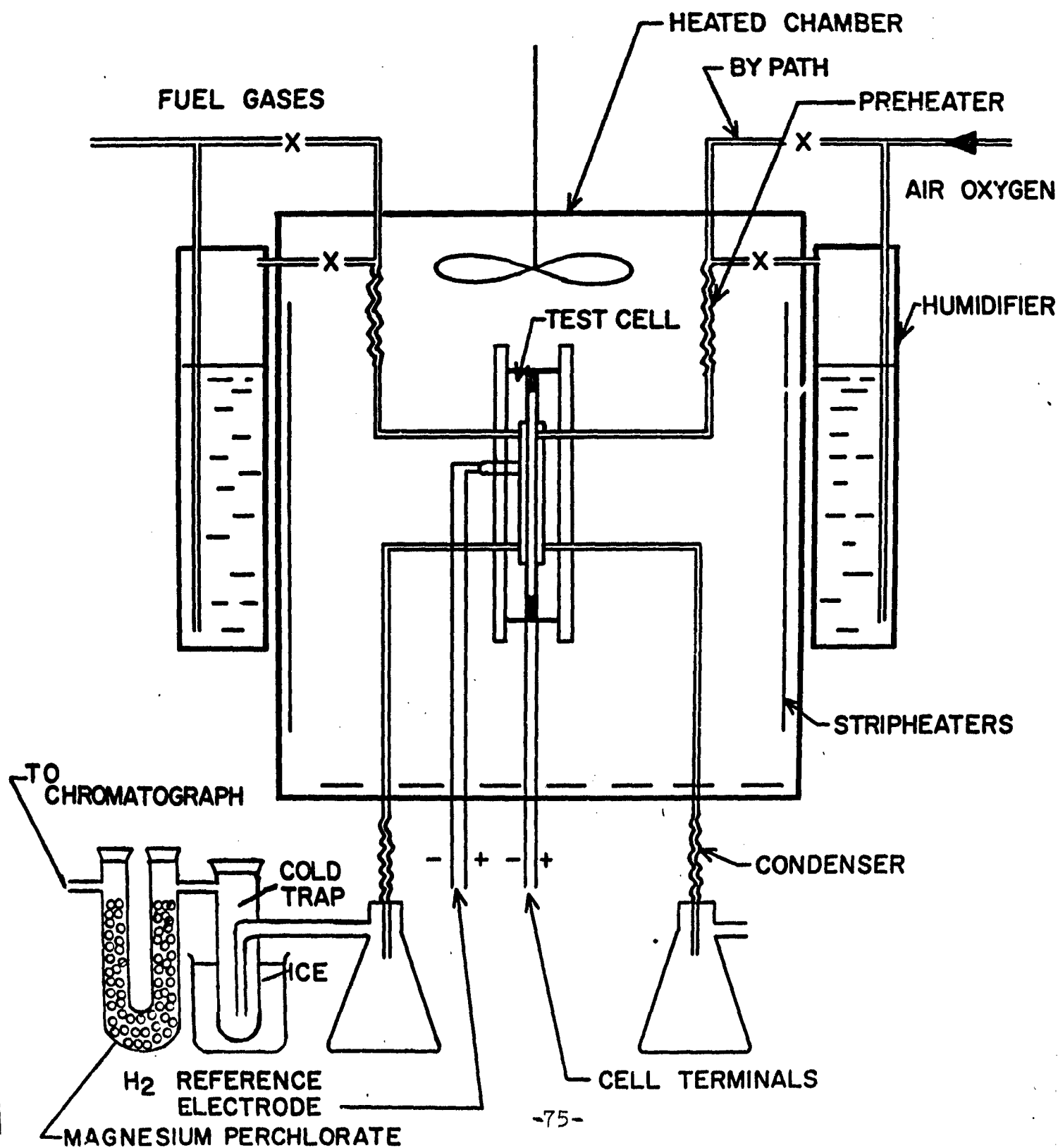


FIG. 9

FUEL CELL ARRANGEMENT
FOR CATALYST EVALUATION

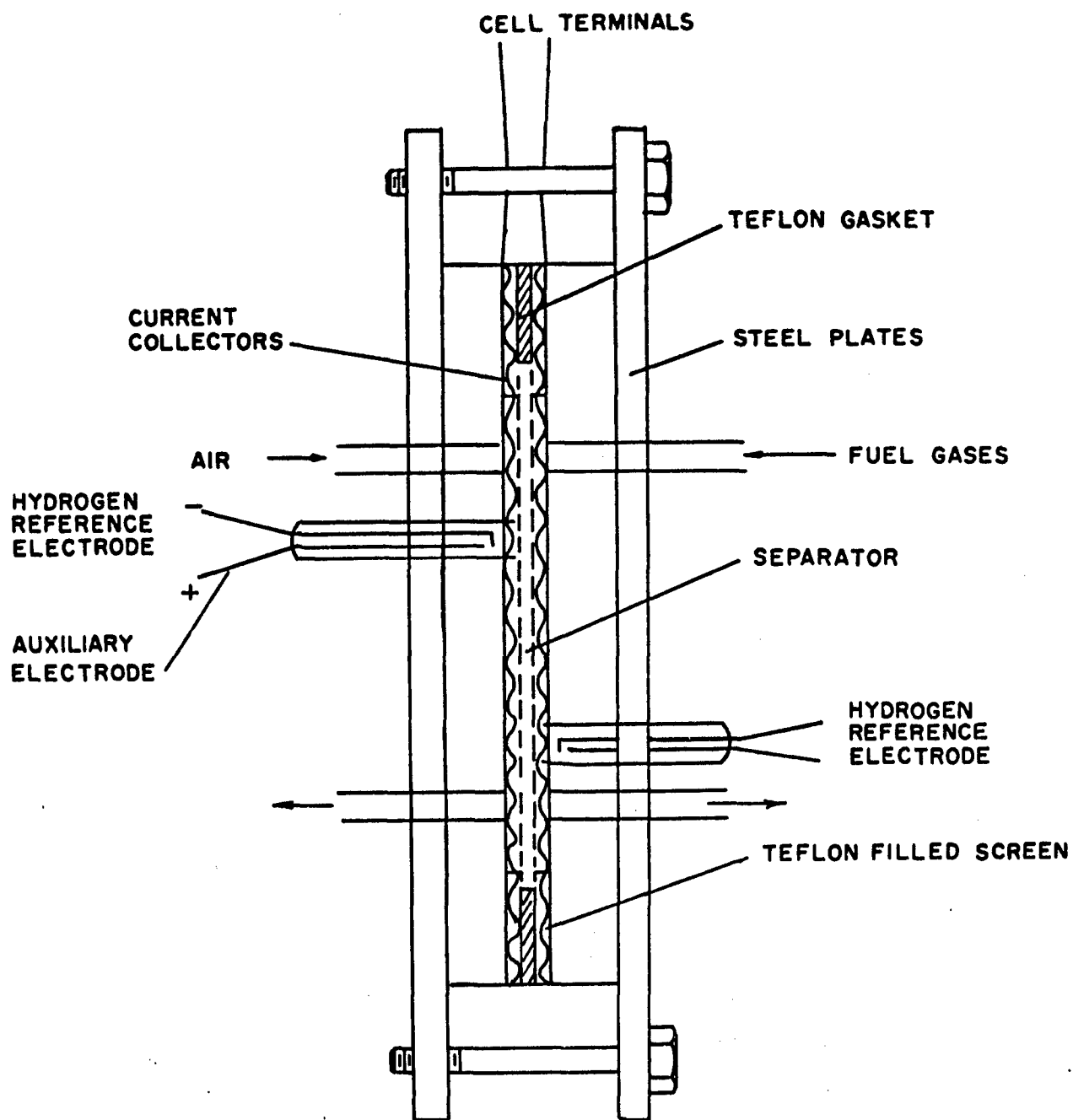


FIG.10
PORE SIZE DISTRIBUTION OF Pt - BLACK

B.E.T. SURFACE AREA : $14 \text{ m}^2/\text{g}$
CRYSTALLITE SIZE : 101 \AA
BULK DENSITY : $.55 \text{ g/cm}^3$

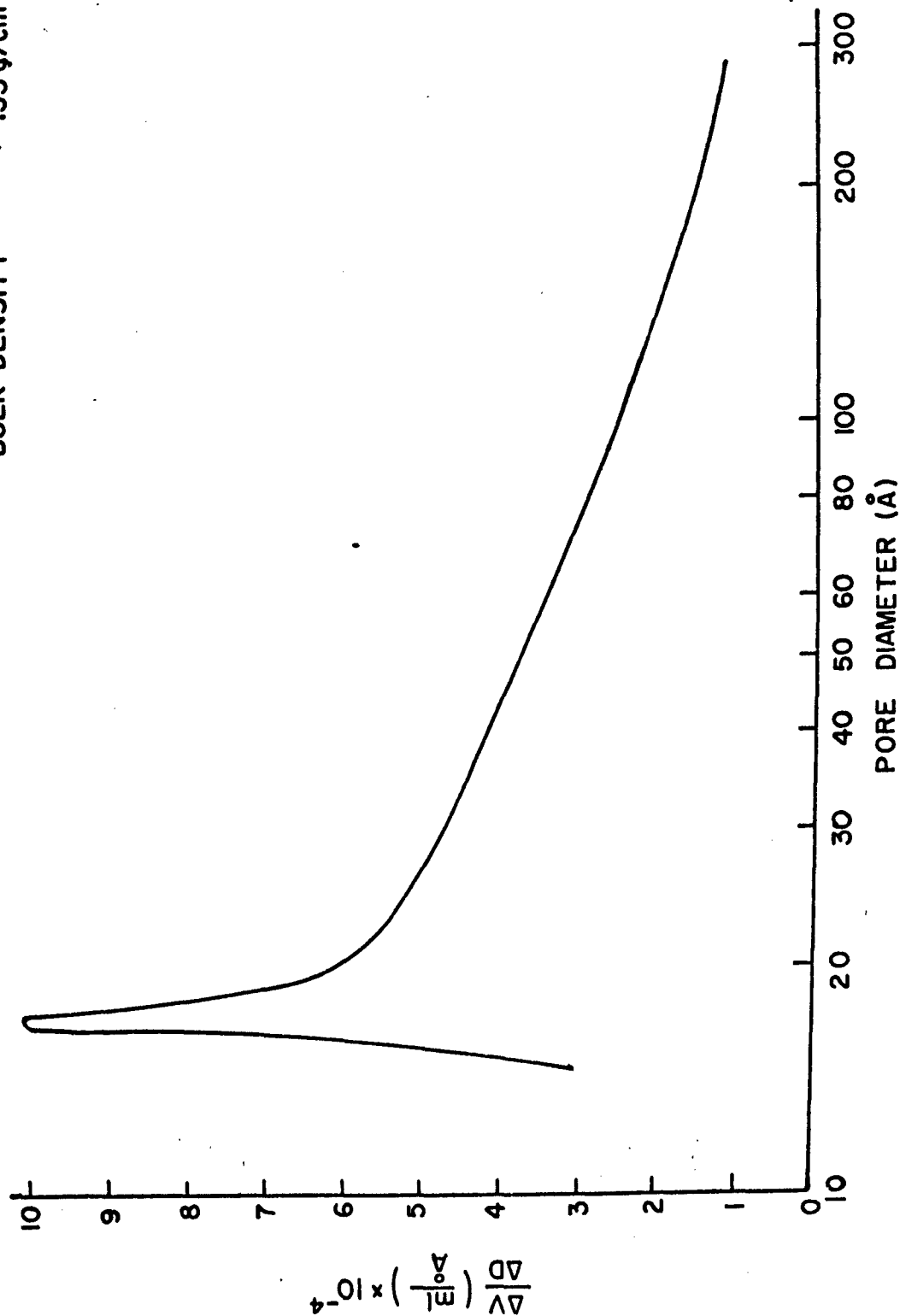


FIG. II

PORE SIZE DISTRIBUTION OF AN IRIIDIUM BLACK CATALYST

B.E.T. SURFACE AREA : 99 m²/g
 X-RAY CRYSTALLITE SIZE : 16 Å
 BULK DENSITY : 2.07 g/cm³

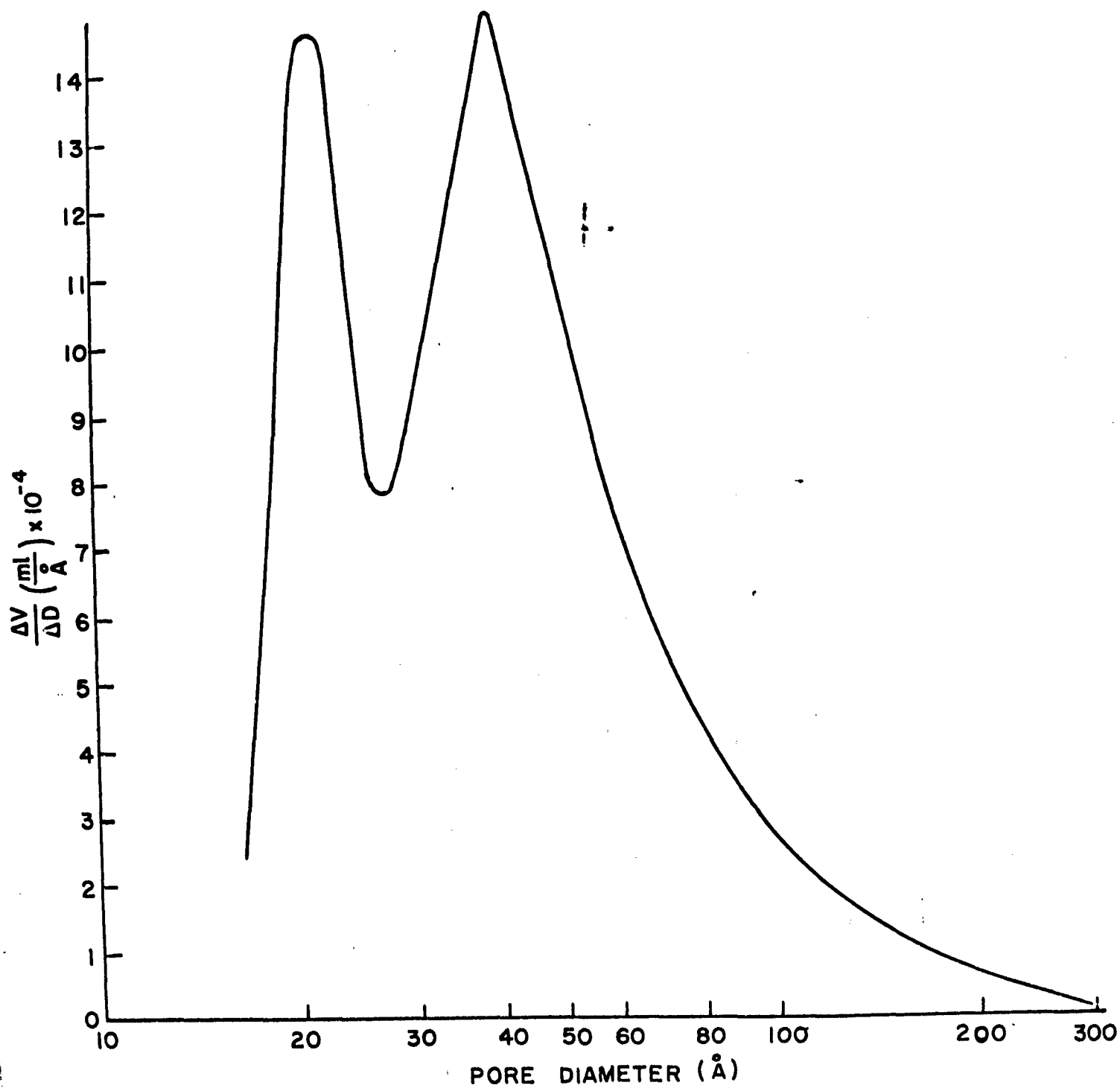


FIG. 12

CHARACTERISTICS OF Pt-Ru CATALYSTS AS FUNCTIONS OF Ru-CONTENT

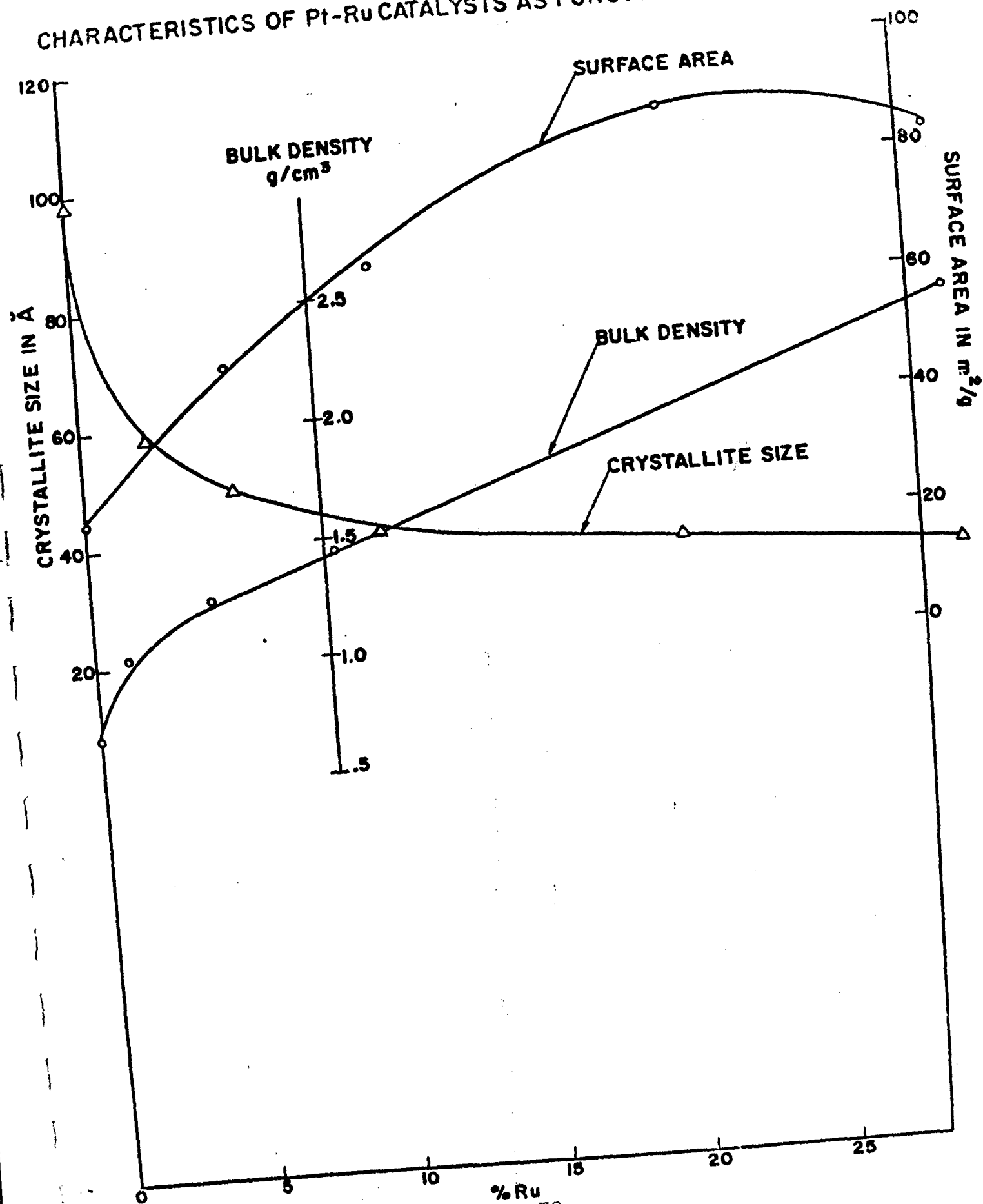


FIG. 13

PORE SIZE DISTRIBUTION OF Pt(99)Ru(1) ALLOY CATALYST

B.E.T. SURFACE AREA : $37.5 \text{ m}^2/\text{g}$
CRYSTALLITE SIZE : 54 \AA
BULK DENSITY : 1.05 g/cm^3

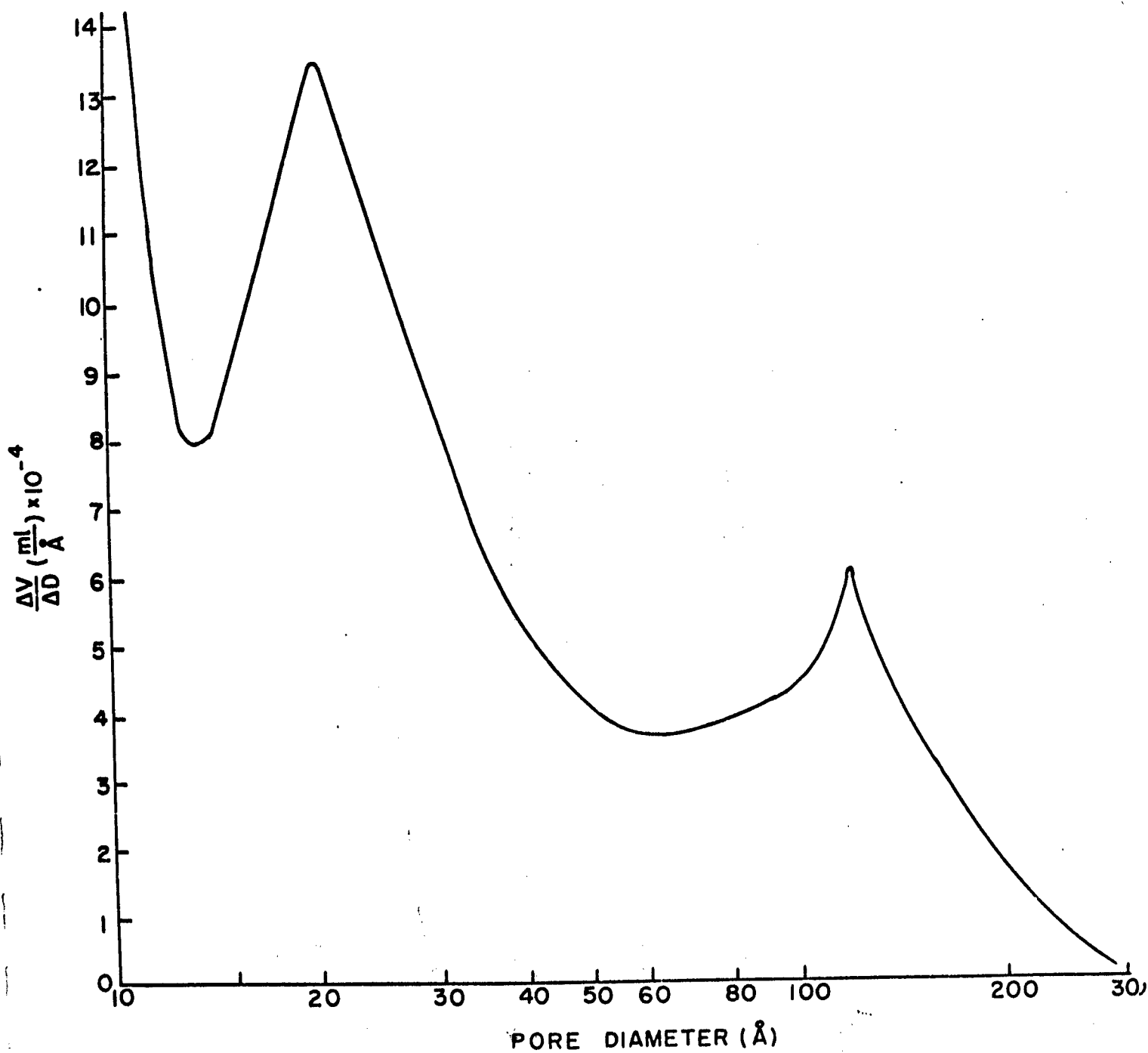


FIG.14

PORE SIZE DISTRIBUTION OF A Pt(95)Ru(5)ALLOY
CATALYST

B.E.T. SURFACE AREA : $48 \text{ m}^2/\text{g}$
X-RAY CRYSTALLITE SIZE : 45 \AA
BULK DENSITY : 1.09 g/cm^3

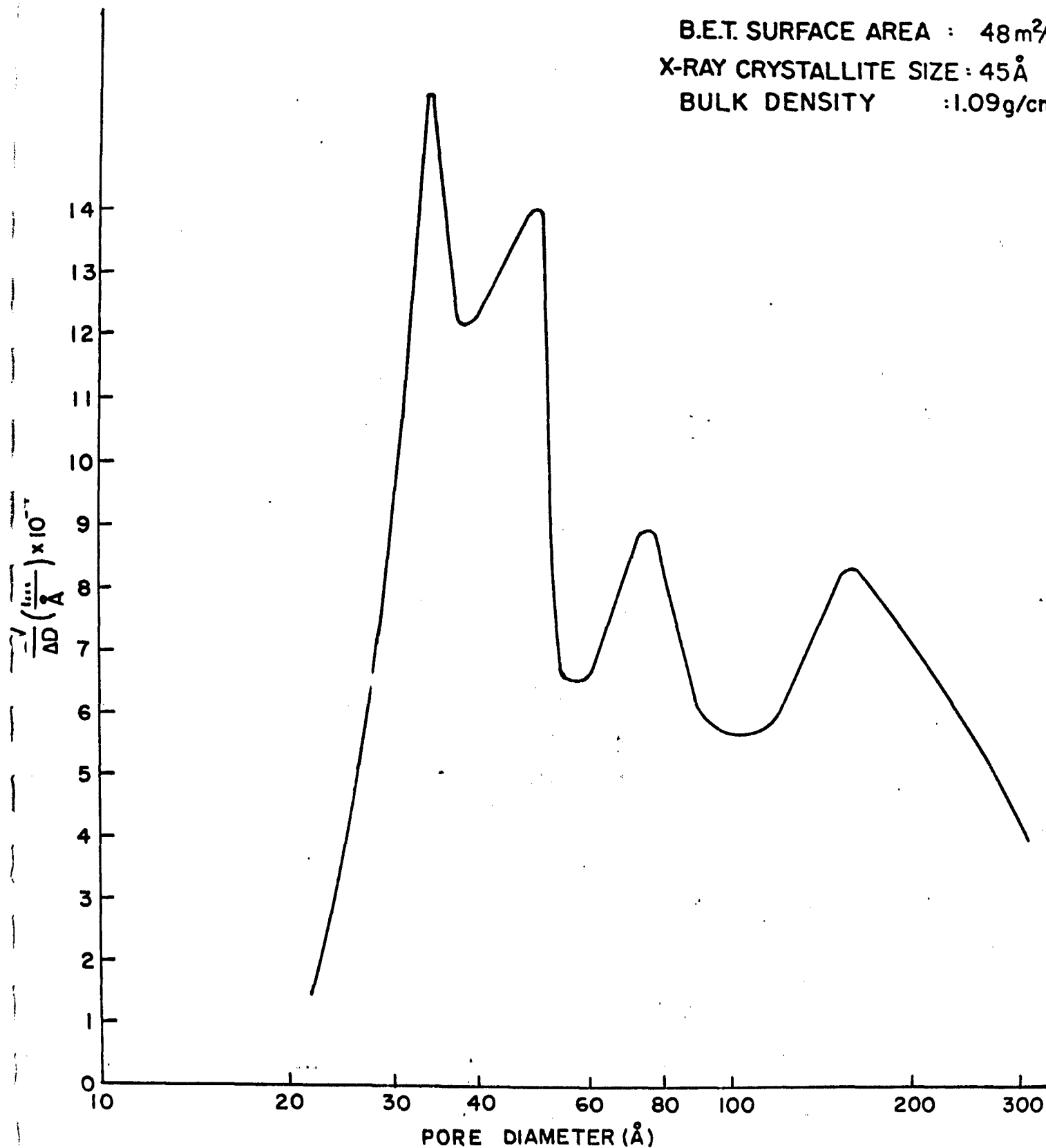


FIG. 15
PORE SIZE DISTRIBUTION OF A Pt(95)Rh(5)
ALLOY CATALYST

B.E.T. SURFACE AREA : $43 \text{ m}^2/\text{g}$
X-RAY CRYSTALLITE SIZE : 47 \AA
BULK DENSITY : $.83 \text{ g/cm}^3$

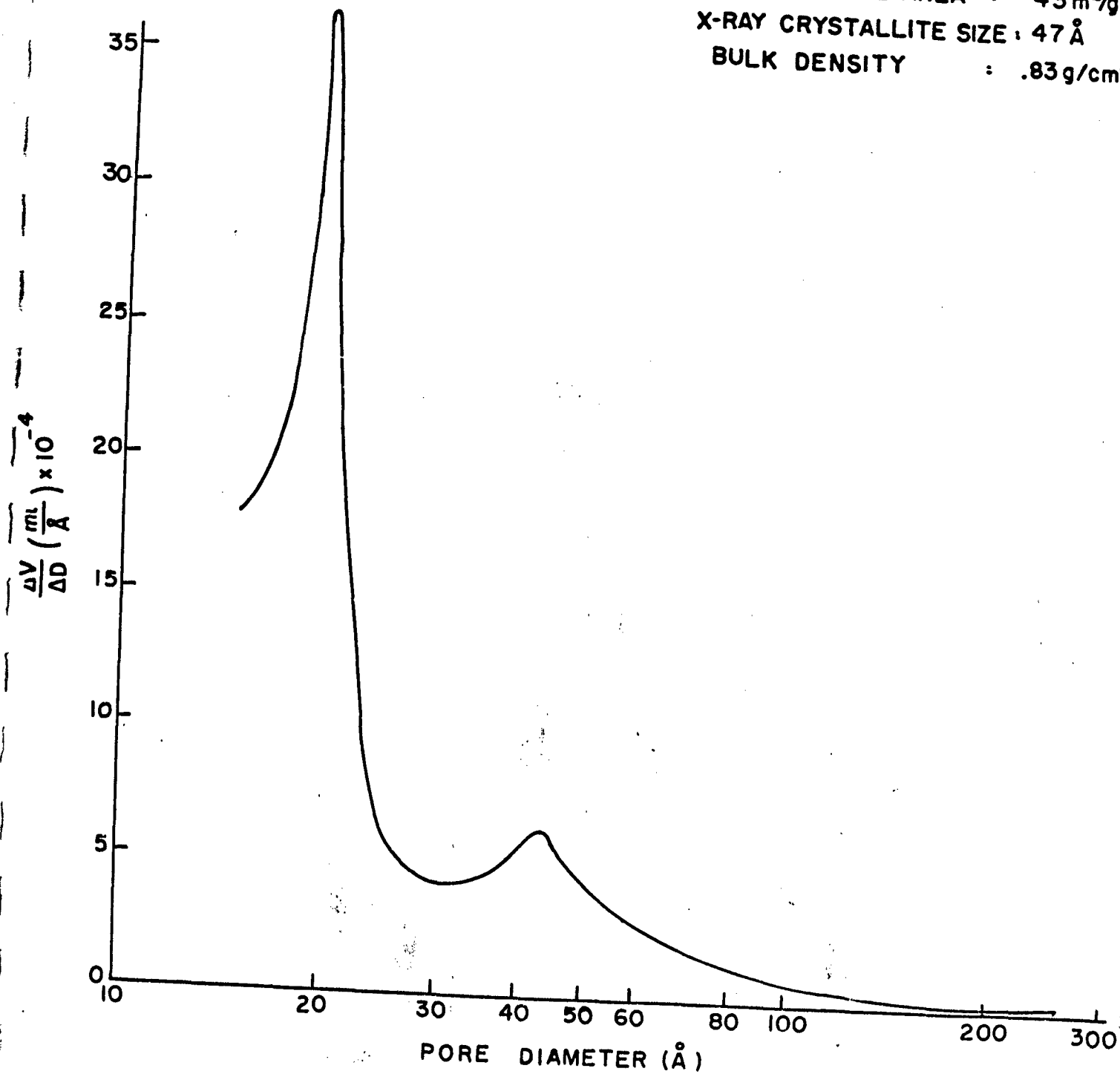


FIG. 16

OXIDATION POTENTIALS OF METHANOL AND PROPANE
AS FUNCTION OF Ru CONTENT IN Ru Pt CATALYSTS

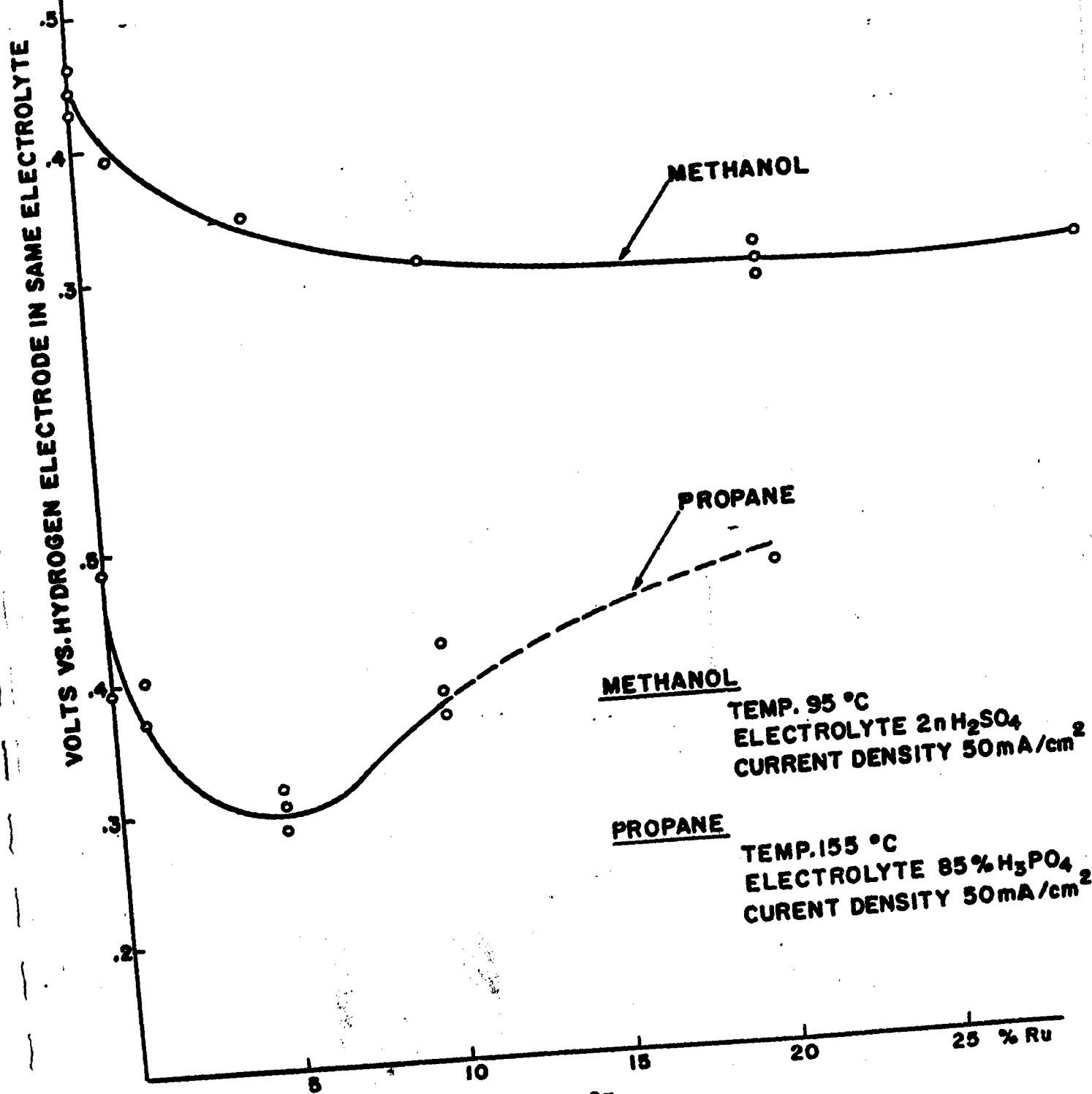
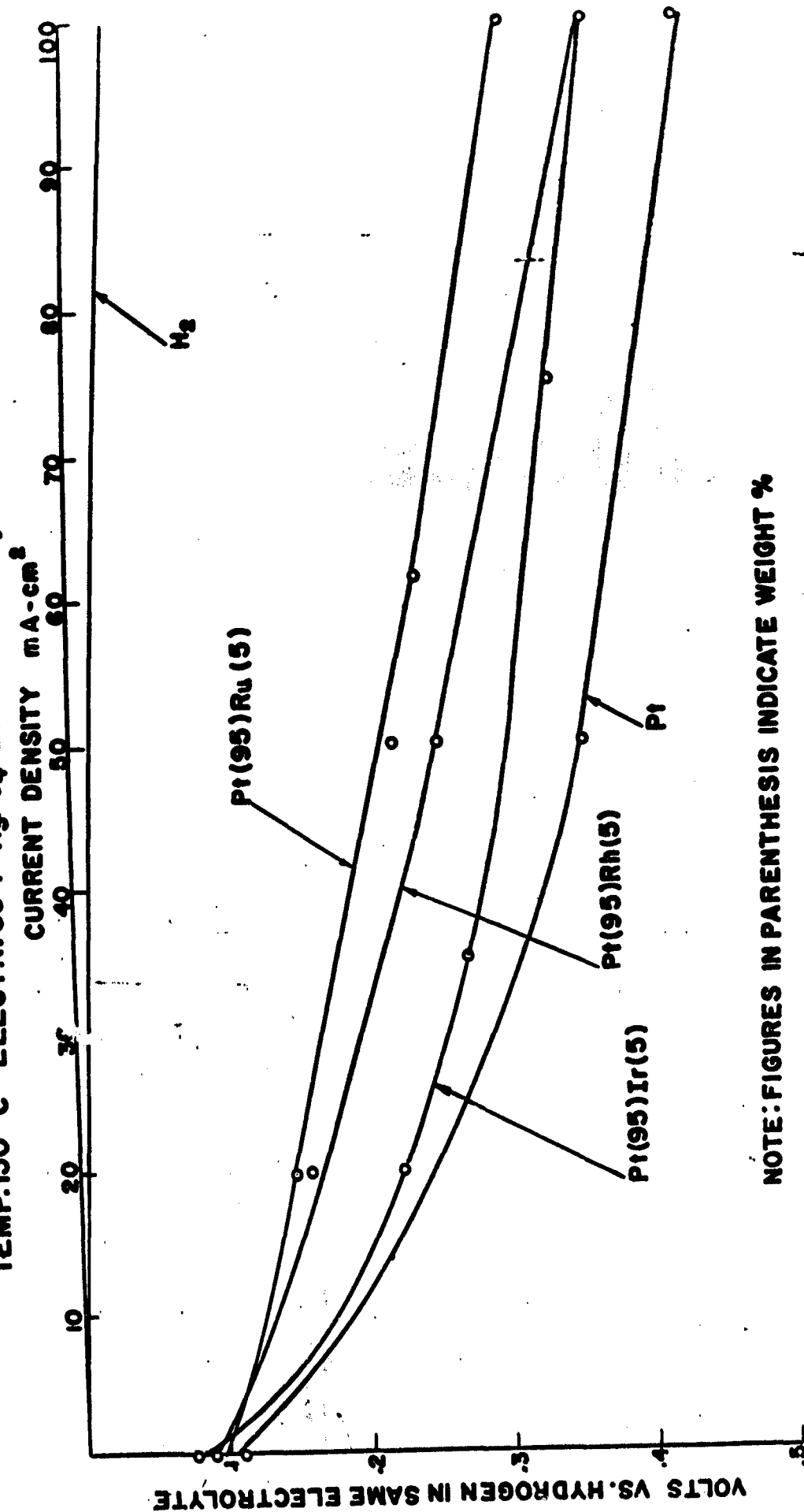


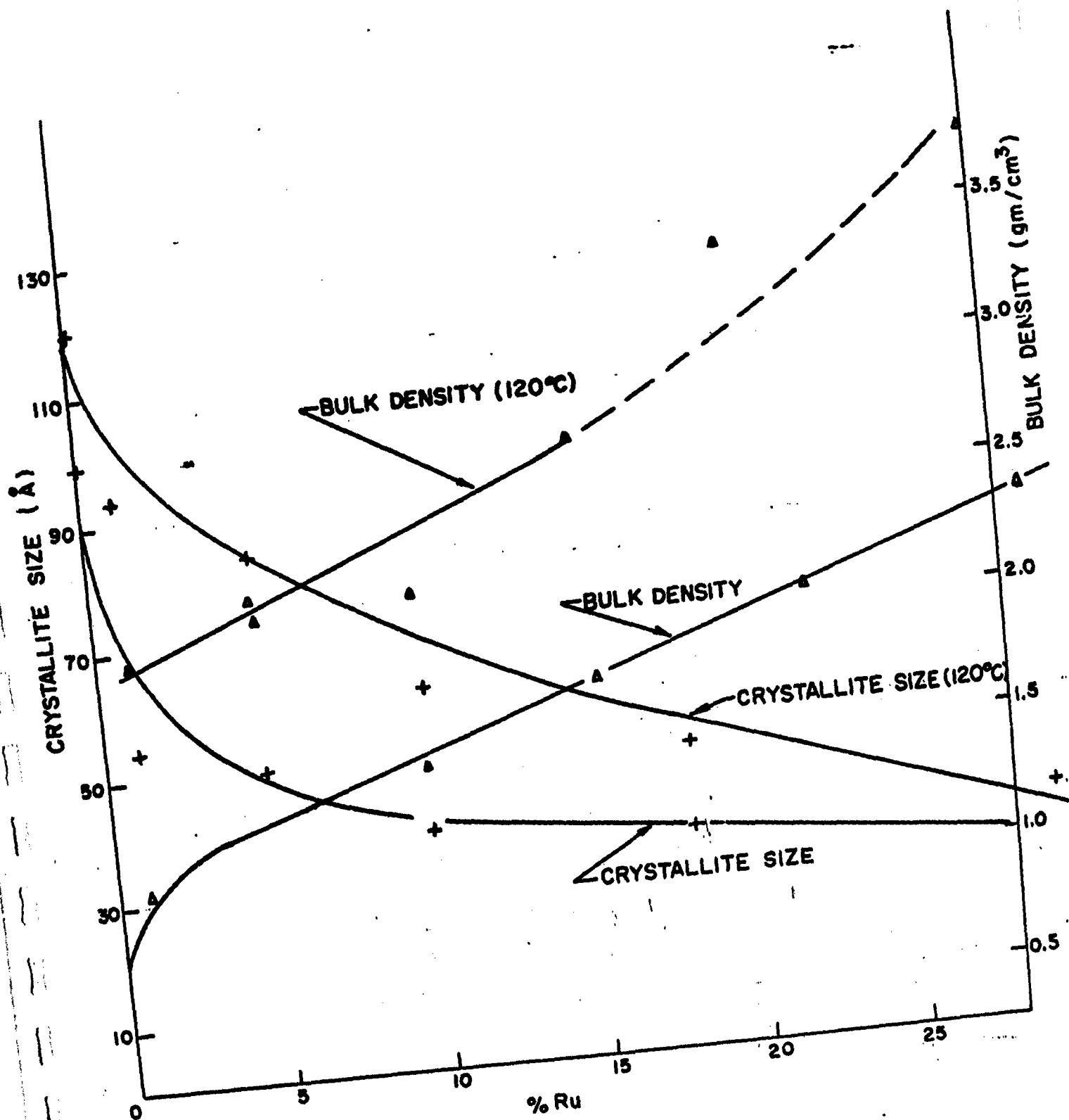
FIG.17

PROPANE OXIDATION ON UNSUPPORTED Pt AND Pt ALLOY CATALYSTS
TEMP.150°C ELECTRO.85 % H_3PO_4 LOADINGS 50 mg./cm^2 ATM.PRESSURE



NOTE: FIGURES IN PARENTHESIS INDICATE WEIGHT %

FIG.18
THERMAL AGING OF Pt-Ru CATALYSTS



lated to the "accessible surface" area. All variations of activity could be associated with the surface area development, and no other effect of primary crystallite size on activity found.

Platinum-ruthenium alloys which have high surface areas and favorable pore structures exhibit markedly superior activity over platinum for the oxidation of methanol, ethane, propane and butene.

Gas chromatographic measurements showed complete oxidation to carbon dioxide of ethane, propane and butene. With ethylene, however, a small amount of carbon monoxide was also formed.

The catalytic metal may be diluted by supporting it on a suitable carrier which may increase activity and stability. A small particle size and low porosity of the carrier is desirable for improved mass transfer.

lated to the "accessible surface" area. All variations of activity could be associated with the surface area development, and no other effect of primary crystallite size on activity found.

Platinum-ruthenium alloys which have high surface areas and favorable pore structures exhibit markedly superior activity over platinum for the oxidation of methanol, ethane, propane and butene.

Gas chromatographic measurements showed complete oxidation to carbon dioxide of ethane, propane and butene. With ethylene, however, a small amount of carbon monoxide was also formed.

The catalytic metal may be diluted by supporting it on a suitable carrier which may increase activity and stability. A small particle size and low porosity of the carrier is desirable for improved mass transfer.

lated to the "accessible surface" area. All variations of activity could be associated with the surface area development, and no other effect of primary crystallite size on activity found.

Platinum-ruthenium alloys which have high surface areas and favorable pore structures exhibit markedly superior activity over platinum for the oxidation of methanol, ethane, propane and butene.

as chromatographic measurements showed complete oxidation to carbon dioxide of ethane, propane and butene. With ethylene, however, a small amount of carbon monoxide was also formed.

The catalytic metal may be diluted by supporting it on a suitable carrier which may increase activity and stability. A small particle size and low porosity of the carrier is desirable for improved mass transfer.

lated to the "accessible surface" area. All variations of activity could be associated with the surface area development, and no other effect of primary crystallite size on activity found.

Platinum-ruthenium alloys which have high surface areas and favorable pore structures exhibit markedly superior activity over platinum for the oxidation of methanol, ethane, propane and butene.

Gas chromatographic measurements showed complete oxidation to carbon dioxide of ethane, propane and butene. With ethylene, however, a small amount of carbon monoxide was also formed.

The catalytic metal may be diluted by supporting it on a suitable carrier which may increase activity and stability. A small particle size and low porosity of the carrier is desirable for improved mass transfer.

Engelhard Industries, Inc.
Research & Development Division
Newark 5, New Jersey
FINAL REPORT NO. 4 by
O. J. Adhart and M.M. Hartwig,
December 1, 1963 to November 30, 1964,
85 pp. incl. illus.
(Task No. 1G6 22001 A 053-04)
Contract DA-36-039 AMC-03700 (E)

UNCLASSIFIED REPORT

A research program is carried out on electrode catalysts for fuel cells employing liquid organic fuels. Complete oxidation of the fuel to carbon dioxide and water is required under expulsion of these products from the fuel cell. The electrolyte, therefore, must be of sufficient acidity to avoid retention of carbon dioxide.

Work under this contract concerned the relationship between activity and structural factors of precious metal catalysts. Catalysts considered were platinum, iridium, rhodium, and platinum alloys with ruthenium, rhodium or iridium.

Aside from intrinsic factors catalytic activity is re-
(over)

Engelhard Industries, Inc.
Research & Development Division
Newark 5, New Jersey
FINAL REPORT NO. 4 by
O. J. Adhart and M.M. Hartwig,
December 1, 1963 to November 30, 1964,
85 pp. incl. illus.
(Task No. 1G6 22001 A 053-04)
Contract DA-36-039 AMC-03700 (E)

UNCLASSIFIED REPORT

A research program is carried out on electrode catalysts for fuel cells employing liquid organic fuels. Complete oxidation of the fuel to carbon dioxide and water is required under expulsion of these products from the fuel cell. The electrolyte, therefore, must be of sufficient acidity to avoid retention of carbon dioxide.

Work under this contract concerned the relationship between activity and structural factors of precious metal catalysts. Catalysts considered were platinum, iridium, rhodium, and platinum alloys with ruthenium, rhodium or iridium.

Aside from intrinsic factors catalytic activity is re-
(over)

UNCLASSIFIED
1. Electric power supply
by fuel cell
2. Complete oxidation of
organic fuels.
3. Electrode catalysts for
oxygen and organic
fuels in carbon dioxide
expellent medium.

I L. Adhart, O.J.
Hartwig, M. M.
II. U.S. Army Electronics
Laboratories
III. Contract DA-36-039
AMC-03700 (E)

Engelhard Industries, Inc.
Research & Development Division
Newark 5, New Jersey
FINAL REPORT NO. 4 by
O. J. Adhart and M.M. Hartwig,
December 1, 1963 to November 30, 1964,
85 pp. incl. illus.
(Task No. 1G6 22001 A 053-04)
Contract DA-36-039 AMC-03700 (E)

UNCLASSIFIED REPORT

A research program is carried out on electrode catalysts for fuel cells employing liquid organic fuels. Complete oxidation of the fuel to carbon dioxide and water is required under expulsion of these products from the fuel cell. The electrolyte, therefore, must be of sufficient acidity to avoid retention of carbon dioxide.

Work under this contract concerned the relationship between activity and structural factors of precious metal catalysts. Catalysts considered were platinum, iridium, rhodium, and platinum alloys with ruthenium, rhodium or iridium.

Aside from intrinsic factors catalytic activity is re-
(over)

Engelhard Industries, Inc.
Research & Development Division
Newark 5, New Jersey
FINAL REPORT NO. 4 by
O. J. Adhart and M.M. Hartwig,
December 1, 1963 to November 30, 1964,
85 pp. incl. illus.
(Task No. 1G6 22001 A 053-04)
Contract DA-36-039 AMC-03700 (E)

UNCLASSIFIED REPORT

A research program is carried out on electrode catalysts for fuel cells employing liquid organic fuels. Complete oxidation of the fuel to carbon dioxide and water is required under expulsion of these products from the fuel cell. The electrolyte, therefore, must be of sufficient acidity to avoid retention of carbon dioxide.

Work under this contract concerned the relationship between activity and structural factors of precious metal catalysts. Catalysts considered were platinum, iridium, rhodium, and platinum alloys with ruthenium, rhodium or iridium.

Aside from intrinsic factors catalytic activity is re-
(over)

UNCLASSIFIED
1. Electric power supply
by fuel cell.
2. Complete oxidation of
organic fuels.
3. Electrode catalysts for
oxygen and organic
fuels in carbon dioxide
expellent medium.

I L. Adhart, O.J.
Hartwig, M. M.
II. U.S. Army Electronics
Laboratories
III. Contract DA-36-039
AMC-03700 (E)

UNCLASSIFIED
1. Electric power supply
by fuel cell.
2. Complete oxidation of
organic fuels.
3. Electrode catalysts for
oxygen and organic
fuels in carbon dioxide
expellent medium.

I L. Adhart, O.J.
Hartwig, M. M.
II. U.S. Army Electronics
Laboratories
III. Contract DA-36-039
AMC-03700 (E)

lated to the "accessible surface" area. All variations of activity could be associated with the surface area development, and no other effect of primary crystallite size on activity found.

Platinum-ruthenium alloys which have high surface areas and favorable pore structures exhibit markedly superior activity over platinum for the oxidation of methanol, ethane, propane and butene.

Gas chromatographic measurements showed complete oxidation to carbon dioxide of ethane, propane and butene. With ethylene, however, a small amount of carbon monoxide was also formed.

The catalytic metal may be diluted by supporting it on a suitable carrier which may increase activity and stability. A small particle size and low porosity of the carrier is desirable for improved mass transfer.

lated to the "accessible surface" area. All variations of activity could be associated with the surface area development, and no other effect of primary crystallite size on activity found.

Platinum-ruthenium alloys which have high surface areas and favorable pore structures exhibit markedly superior activity over platinum for the oxidation of methanol, ethane, propane and butene.

Gas chromatographic measurements showed complete oxidation to carbon dioxide of ethane, propane and butene. With ethylene, however, a small amount of carbon monoxide was also formed.

The catalytic metal may be diluted by supporting it on a suitable carrier which may increase activity and stability. A small particle size and low porosity of the carrier is desirable for improved mass transfer.

lated to the "accessible surface" area. All variations of activity could be associated with the surface area development, and no other effect of primary crystallite size on activity found.

Platinum-ruthenium alloys which have high surface areas and favorable pore structures exhibit markedly superior activity over platinum for the oxidation of methanol, ethane, propane and butene.

Gas chromatographic measurements showed complete oxidation to carbon dioxide of ethane, propane and butene. With ethylene, however, a small amount of carbon monoxide was also formed.

The catalytic metal may be diluted by supporting it on a suitable carrier which may increase activity and stability. A small particle size and low porosity of the carrier is desirable for improved mass transfer.

lated to the "accessible surface" area. All variations of activity could be associated with the surface area development, and no other effect of primary crystallite size on activity found.

Platinum-ruthenium alloys which have high surface areas and favorable pore structures exhibit markedly superior activity over platinum for the oxidation of methanol, ethane, propane and butene.

Gas chromatographic measurements showed complete oxidation to carbon dioxide of ethane, propane and butene. With ethylene, however, a small amount of carbon monoxide was also formed.

The catalytic metal may be diluted by supporting it on a suitable carrier which may increase activity and stability. A small particle size and low porosity of the carrier is desirable for improved mass transfer.

DISTRIBUTION LIST
FINAL REPORT
CONTRACT NO. DA 36-039 AMC-03700(E)

Director U.S.A. Electronics Laboratories Fort Monmouth, N.J. 07703 ATTN: Logistics Division (Marked For Project Engineer)	(2)	Deputy President U.S.A. Security Agency Board Arlington Hall Station Arlington 12, Virginia	(1)
ATTN: AMSEL-RD-P	(1)	Commander Defense Documentation Center	
ATTN: AMSEL- RD-ADO-RHA	(1)	ATTN: TISIA	
ATTN: AMSEL-RD-DR	(1)	Cameron Station, Building 5	
ATTN: Technical Documents Center	(1)	Alexandria, Virginia 22314	(19)
OASD (Research & Engineering) ATTN: Technical Library Room 3E1065 The Pentagon Washington 25, D.C.	(1)	Chief U.S.A. Security Agency ATTN: ACofS, G-4 (Tech Library) Arlington Hall Station Arlington 12, Virginia	(2)
Chief of Research & Development OCS, Department of the Army Washington 25, D.C.	(2)	Air Force Cambridge Research Lab. ATTN: CRXL-R L. G. Hanscom Field Bedford, Massachusetts	(1)
Commanding General U.S.A. Electronics Command ATTN: AMSEL-TE Fort Monmouth, N.J. 07703	(1)	Headquarters U.S.A. Material Command Research & Development Directorate ATTN: AMCRD-DE-MO Washington, D.C. 20315	(1)
Director U.S. Naval Research Laboratory ATTN: Code 2027 Washington, D.C. 20390	(1)	Commander U.S. Army Research Office (Durham) Box CM-Duke Station Durham, North Carolina	(1)
Commanding Officer & Director U.S. Naval Electronics Laboratory ATTN: Library San Diego 52, California	(1)	Commanding Officer U.S.A. Combat Developments Command ATTN: CDCMR-E Fort Belvoir, Virginia 22060	(1)
Home Air Development Center ATTN: RAALD Griffiss Air Force Base, N.Y.	(1)	Commanding Officer U.S.A. Combat Development Command Communications-Electronic Agency Building 426 Fort Monmouth, N.J. 07703	(1)
Commanding General U.S.A. Electronics Research & Development Activity Fort Huachuca, Arizona 85613	(1)	Air Force Systems Command Scientific Technical Liaison Office U.S. Naval Air Development Center Johnsville, Pennsylvania	(1)
Commanding Officer Harry Diamond Laboratories Connecticut Ave. & Van Ness St., N.W. Washington 25, D.C.	(1)	Director U.S.A. Engineering Research & Development Laboratories ATTN: Chief, Electric Power Branch Fort Belvoir, Virginia 22060	(1)
Director Proc & Prod Directorate ATTN: Technical Library U.S.A. Electronics Command Fort Monmouth, N.J. 07703	(1)		

Marine Corps Liaison Office U.S.A. Electronics Laboratories ATTN: AMSEL-RD-LNR Fort Monmouth, N.J. 07703	(1)	Headquarters U.S.A. Material Command Research & Development Directorate ATTN: AMCFD-RC-P Washington, D.C. 20315	(1)
AFSC Scientific Technical Liaison Office U.S.A. Electronics Laboratories ATTN: AMSEL-RD-LNA Fort Monmouth, N.J. 07703	(1)	Dr. Bernard Stein Physical Sciences Division Army Research Office 3045 Columbia Pike Arlington, Virginia	(1)
USAEEL Liaison Office Rome Air Development Center ATTN: RAOL Griffiss Air Force Base, N.Y. 13442	(1)	Dr. Ralph Roberts Head, Power Branch Office of Naval Research (Code 429) Department of the Navy Washington, D.C. 20360	(1)
Commanding Officer U.S.A. Engineer Research & Develop- ment Laboratories ATTN: STINFO Branch Fort Belvoir, Virginia 22060	(2)	Mr. Bernard B. Rosenbaum Bureau of Ships (Code 342B) Department of the Navy Washington 25, D.C.	(1)
Commanding Officer U.S.A. Electronics Research & Development Activity ATTN: AMSEL-RD-WS-A White Sands, New Mexico 88002	(1)	Mr. George W. Sherman Aerospace Power Division ATTN: API Wright-Patterson Air Force Base Ohio 45433	(1)
NASA Representative Scientific & Technical Information Facility P.O. Box 5700 Bethesda, Maryland 20014	(1)	Mr. M. Polk Advanced Research Projects Agency The Pentagon, Room 3E157 Washington 25, D.C.	(1)
Power Information Center Moore School Building 800 South Thirty-Third Street Philadelphia, Pennsylvania 19103	(1)	Lt. Col. John H. Andersen SNAP-50/SPUR Office U.S. Atomic Energy Commission Division of Reactor Development Washington, D.C. 20545	(1)
Commanding General U.S. Army Material Command ATTN: R & D Directorate Washington, D.C. 20315	(2)	Mr. E. Cohn National Aeronautics & Space Administration Headquarters Code RNW Washington, D.C. 20546	(1)
Systems Engineering Group (SEPIR) Wright-Patterson Air Force Base Ohio 45433	(1)	Institute for Defense Analysis 1666 Connecticut Ave., N.W. Washington 25, D.C. ATTN: Dr. Szegel & Mr. Hamilton	(1)
Electronic Systems Division (AFSC) Scientific & Technical Information Division (ESTI) L. G. Hanscom Field Bedford, Massachusetts 01731	(1)	Mr. G. B. Wareham Office of Assistant Director Defense Research & Engineering 3D-1048 Pentagon Washington 25, D.C.	(1)
Director Material Readiness Directorate HQ, U.S.A. Electronics Command ATTN: AMSEL-MR Fort Monmouth, N.J. 07703	(1)		

United Aircraft Corporation
Pratt & Whitney Aircraft Division
East Hartford 8, Connecticut
ATTN: Mr. W. H. Podolny

(1)

Helpar, Inc.
5000 Arlington Boulevard
Falls Church, Virginia
ATTN: Mr. R. T. Foley

(1)

General Electric Company
Direct Energy Conversion Operations
Lynn, Massachusetts
ATTN: Dr. E. Oster

(1)

General Electric Company
Research Laboratory
Schenectady, New York
ATTN: Dr. H. Liebhafsky

(1)

Esso Research & Engineering Co.
Products Research Division
P.O. Box 215
Linden, New Jersey
ATTN: Dr. W. Epperly

(1)

University of Pennsylvania
John Harrison Laboratory of Chemistry
Philadelphia 4, Pennsylvania
ATTN: Dr. J. Bockris

(1)

Westinghouse Electric Corporation
3 West Front Street
Red Bank, New Jersey
ATTN: Mr. C. Arthur

(1)

Alagna Corporation
R & D Laboratories
1001 South East Street
Anaheim, California
ATTN: Dr. Silverman

(1)

TV Research Center
P.O. Box 5003
Dallas 22, Texas
ATTN: Mr. H. B. Gibbons

(1)

American Oil Company
Research & Development Department
Refining Laboratories
2500 New York Avenue
P.O. Box 431
Refining, Indiana

(1)

University of California
Chemistry Department
Berkeley, California
ATTN: Dr. C. Tobias

Union Carbide Corporation
Parma Research Center
P.O. Box 6136
Parma 30, Ohio
ATTN: Dr. E. E. Winters

(1)

Electrochimica Corporation
1140 O'Brien Drive
Menlo Park, California
ATTN: Dr. M. Eisenberg

(1)

Allis-Chalmers Manufacturing Co.
Research Division
P.O. Box 512
Milwaukee, Wisconsin
ATTN: Dr. P. Joyner

(1)

Allison Division
General Motors Corporation
P.O. Box 894
Indianapolis 6, Indiana
ATTN: Dr. R. E. Henderson

(1)

Texas Instruments, Inc.
Energy Research Laboratory
P.O. Box 5474
Dallas 22, Texas
ATTN: Dr. G. G. Peattie

(1)

P. R. Mallory & Company, Inc.
Technical Services Laboratory
Indianapolis, Indiana
ATTN: Mr. A. S. Doty

(1)